

OPEN ACCESS

EDITED BY Yunyun Zhuang, Ocean University of China, China

REVIEWED BY
Shailesh Nair,
Chinese Academy of Sciences (CAS), China
Yoonja Kang,
Chonnam National University,
Republic of Korea

*CORRESPONDENCE Steven W. Wilhelm ☑ wilhelm@utk.edu

[†]These authors have contributed equally to this work

RECEIVED 30 April 2024 ACCEPTED 05 August 2024 PUBLISHED 21 August 2024

CITATION

Truchon AR, Chase EE, Stark AR and Wilhelm SW (2024) The diel disconnect between cell growth and division in *Aureococcus* is interrupted by giant virus infection.

Front. Microbiol. 15:1426193. doi: 10.3389/fmicb.2024.1426193

COPYRIGHT

© 2024 Truchon, Chase, Stark and Wilhelm. This is an open-access article distributed under the terms of the Creative Commons Attribution License (CC BY). The use, distribution or reproduction in other forums is permitted, provided the original author(s) and the copyright owner(s) are credited and that the original publication in this journal is cited, in accordance with accepted academic practice. No use, distribution or reproduction is permitted which does not comply with these terms.

The diel disconnect between cell growth and division in *Aureococcus* is interrupted by giant virus infection

Alexander R. Truchon[†], Emily E. Chase[†], Ashton R. Stark and Steven W. Wilhelm*

Department of Microbiology, University of Tennessee, Knoxville, TN, United States

Viruses of eukaryotic algae have become an important research focus due to their role(s) in nutrient cycling and top-down control of algal blooms. Omicsbased studies have identified a boom of genomic and transcriptional potential among the Nucleocytoviricota, a phylum of large dsDNA viruses which have been shown to infect algal and non-algal eukaryotes. However, little is understood regarding the infection cycle of these viruses, particularly in how they take over a metabolically active host and convert it into a virocell state. Of particular interest are the roles light and the diel cycle play in virocell development. Yet despite such a large proportion of Nucleocytoviricota infecting phototrophs, little work has been done to tie infection dynamics to the presence, and absence, of light. Here, we examined the role of the diel cycle on the physiological and transcriptional state of the pelagophyte Aureococcus anophagefferens while undergoing infection by Kratosvirus quantuckense strain AaV through flow cytometry and differential expression analyses. Our observations demonstrate how infection by the virus interrupts the diel growth and division of this cell strain, and that infection further complicates the system by enhancing export of cell biomass. Furthermore, these analyses reinforce the expectation that viral activity is heavily associated with the diel cycle.

KEYWORDS

diel periodicity, harmful algal bloom, Nucleocytoviricota, host-virus system, virocell

Introduction

Diel patterns in phytoplankton are common. Specific factors known to cycle on a diel basis (i.e., diel periodicity) among phytoplankton include population density, biomass, community species composition, intracellular metabolism, resources (e.g., nutrients, organic constituents, DNA concentration), enzymatic activity, and primary production (Prezelin, 1992). Early field-based studies acknowledged these diel cycles, and began investigating the influence that time-of-collection for sampling might have on aquatic plankton research (Maxwell and Mikihiko, 1957; Yentsch and Ryther, 1957; Shimada, 1958; Doty, 1959). By the 1960s, green algae, dinoflagellates, and diatoms had all been observed to have diel patterns *in vitro* (Holmes and Haxo, 1958; Hastings et al., 1961). Generally, this diel cycle of phytoplankton has been thought to be decoupled from ambient light (Harding et al., 1981; Yoshikawa and Furuya, 2006). Still, higher resolution of this cycle in various algal systems during experimentation enhances the reproducibility of results. In a cell division periodicity study of 26 clonal cultures of marine algal

cultures (representing 13 species), it was found that intraspecific variation does occur, and that different algal species can exhibit diel periodicity with division occurring at night or during the day (Nelson and Brand, 1979). For example, it was found that in phytoplankton collected from Sagami Bay (Japan), photosynthetic maxima (normalized absorption; mol C m⁻² h⁻¹) were highest at noon, and lower at dawn and dusk, with end-of-day timepoints being significantly variable (Yoshikawa and Furuya, 2006). Thus, photosynthetic variations were thought to be endogenously regulated (Behrenfeld et al., 2004). In the polymorphic haptophyte *Phaeocystis pouchetii*, it has been shown that synchronized cell division occurs midway through the dark cycle (on a 12/12 light: dark cycle), and that at higher light intensities or longer light cycles, cells could experience a division rate of greater than once per day (Jacobsen and Veldhuis, 2005).

Recent examinations of diel periodicity have focused on the functional roles and dynamics of important marine microbes, which has been given further context through new methods including metatranscriptomics and flow cytometry (Aylward et al., 2015; Hu et al., 2018; Henderikx Freitas et al., 2020). Many studies have explored the implications of diel periodicity in Bacteria, Eukaryota, and Archaea in important coastal and open ocean systems (Ottesen et al., 2014; Groussman et al., 2021; Muratore et al., 2022). In the North Pacific Subtropical Gyre, autotrophic metabolism was heightened during the day, and authors found that diel cycles in bacteria (e.g., Synechococcus and Prochlorococcus) included an increase in cell-size during the day, and cell division around dusk (Hu et al., 2018). Other studies have shown that picocyanobacterial gene expression is tied to diel periodicity (Zinser et al., 2009). However, picocyanobacterial cell counts remained stable in the gyre, as their diel metabolic activity was linked with the diel activity of dinoflagellates, haptophytes, ciliates, and marine stramenopiles which would graze on the newly divided cells around dusk. Furthermore, diel periodicity of dominant photoautotrophs (e.g., Ostreococcus and Prochlorococcus) has been shown to shape community dynamics via light-based carbon acquisition at the base of the food web (Poretsky et al., 2009; Aylward et al., 2015). However, there have been few studies exploring important bloom producing algae, nor how viral infection of algae and the formation of a virocell (a cell actively undergoing viral infection and thus with altered metabolic function) are affected by diel cycling. Although viruses were not explored in these studies, it is logical that they would also be influenced by their hosts' reaction to the diel cycle.

In theory, the dominant algae within a system can change during blooms, establishing a new community dynamic still potentially coupled to diel cycles. Such effects could include shifts in populations grazing on a phytoplankton, shifts in primary productivity, and/or changes in light penetration of the water system. Viruses have been demonstrated to be important factors in bloom dynamics and are specifically implicated in bloom termination (Jacquet et al., 2002; Brussaard et al., 2005; Steffen et al., 2017). Their role also has implications for biogeochemical cycling, including open ocean impacts on carbon cycling (i.e., the viral shunt; Wilhelm and Suttle, 1999) and carbon export (i.e., the viral shuttle; Sullivan et al., 2017). Indeed, a recent mesocosm study of carbon release showed viruses drove a 2-to 4-fold increase in extracellular carbon during bloom termination (Vincent et al., 2023). Thus, the effects of bloom events and bloom termination in the context of diel periodicity are important, especially given the diversity of life cycle strategies used by the causative agents of blooms and their viruses.

For the past two decades the brown tide bloom agent Aureococcus anophagefferens and "giant virus" Kratosvirus quantuckense (family Schizomimiviridae) have been studied in detail (Sieburth et al., 1988; Rowe et al., 2008; Truchon et al., 2023). The pelagophyte A. anophagefferens was characterized in 1985 (Sieburth et al., 1988) and has continued to produce blooms along the East Coast of the United States (Narragansett Bay, Barnegat Bay, Long Island bays) (Bricelj and Lonsdale, 1997), off the coast of China (near Qinhuangdao; Bohai Sea) (Zhang et al., 2012) and a bay on the southwest coast of South Africa (Saldanha Bay) (Probyn et al., 2010). Brown tides are designated as harmful algal blooms (HABs) because of their economic and ecological detriment (Gobler et al., 2005). The virus K. quantuckense has been implicated as a regulator of A. anophagefferens brown tide bloom termination via population-wide cell mortality (Gastrich et al., 2004). Notably, irradiance levels have previously been tied to viral burst size in an in vitro setting, demonstrating that virus particles produced during an infection cycle are dependent on the availability of light (Gann et al., 2020a). If light is important to infection, then it is possible that stages of the viral life cycle as well as virocell gene expression are tied to the diel cycle as well. Given the need to better understand the physiological ecology and energetics of brown tides, we monitored the diel periodicity of this brown tide agent alone and during viral infection in lab studies to determine how viral infection can affect the alga's response to light. We observed a strict partitioning of physiological and metabolic processes by A. anophagefferens in relation to diel periodicity that was interrupted by viral infection.

Methods and materials

Culture conditions

Three non-axenic isolates of Aureococcus anophagefferens were studied, including two that are resistant (strains CCMP1850 and CCMP1707) and a third (strain CCMP1984) susceptible to lytic infection by Kratosvirus quantuckense strain AaV (Aureococcus anophagefferens Virus) (Rowe et al., 2008). Cultures were maintained at 19° C under a 12:12 light dark cycle in ASP₁₂A growth media (Gann, 2016). Light levels for maintenance and experimental cultures were $\sim 70\,\mu mol$ photons $m^{-2}\,s^{-1}.$ Shading experiments were conducted by wrapping one or two layers of neutral density screening around individual culture tubes that reduced irradiance to 40 and 20 µmol photons m⁻² s⁻¹, respectfully. Prior to experimentation under reduced light conditions, cultures were moved and acclimated to the specific light treatment for at least 72h. The concentration of cells in A. anophagefferens cultures was determined using a CytoFLEX flow cytometer (Beckman Coulter, Brea, CA) (Chase et al., 2022). Abundance in samples for gated cellular populations was quantified via violet side scatter (V-SSc) versus peridinin-chlorophyll fluorescence (absorption 488 nm, emission 690 nm) (Chase et al., 2022).

Cell diameter estimates

Individual cell diameters were determined based on measurements from a FlowCam 8000 (Fluid Imaging Technologies, Scarborough, ME). Briefly, culture samples were diluted to

approximately 1×10^6 cells ml⁻¹ and then imaged using the FlowCam's 20X objective. Ten thousand individual cellular images were used to calculate average cell diameter and volume as well as for verification of cell concentration (using VisualSpreadsheet 2). FlowCam measurements for average diameter were compared to flow cytometry measurements taken on the V-SSc channel using a 405 nm violet laser (CytoFLEX C07821), an approach which has previously been utilized for estimating cell size in algae and small particles (Chioccioli et al., 2014; McVey et al., 2018). A. anophagefferens CCMP1984 was compared on both devices over the course of 24h after either being infected (see below) or treated with filtered viral lysate. To determine the relation between these measurements, a Pearson's coefficient was calculated. A. anophagefferens CCMP1984 cell diameter determined from the FlowCam 8000 was correlated strongly with the V-SSc measurements (p < 0.001; $R^2 = 0.9413$) (Supplementary Figure S1). This correlation was consistent for both virus-infected and uninfected A. anophagefferens cells through different stages of the growth and infection cycle. For this reason, V-SSc was used as a proxy for average cell diameter for the remainder of the experimentation.

Infection with Kratosvirus quantuckense

The AaV strain of *K. quantuckense* has been maintained in culture since its isolation in 2008 (Rowe et al., 2008). Fresh AaV particles were generated by infection of 1 L of a 7d-old culture of A. anophagefferens CCMP1984 grown in ASP₁₂A medium as above. After allowing the population to lyse (14 d), lysate was filtered sequentially through 1-μm and 0.45-µm pore-size, 47-mm diameter low protein binding Durapore (PVDF) membrane filters (MilliporeSigma; Burlington, MA). Viruses in the filtered lysate were concentrated via tangential flow filtration through a 30 kDa Pelicon XL (MilliporeSigma; Burlington MA) filter to an approximate volume of 50 mL as previously described (Coy and Wilhelm, 2020). Following concentration of viruses from lysate, contaminating bacteria were removed via centrifugation (3,500 \times g, 10 min). Viral particles were enumerated via flow cytometry (Chase et al., 2023). Briefly, lysate was fixed with 1% glutaraldehyde solution in the dark at 4° C for at least 1 h. Lysate was then stained with SYBR Gold (Invitrogen; Waltham, MA) at a final concentration 0.5X at 80° C for 10 min. Virus particles were enumerated using the violet laser on a CytoFLEX flow cytometer (C07821) (Beckman Coulter; Brea, CA) (Chase et al., 2023; Zhao et al., 2023).

For experiments, infection of A. anophagefferens was performed on cells in exponential growth stage diluted to 1×10^6 cells ml $^{-1}$ in fresh $ASP_{12}A$ medium. Viral lysate was added to diluted A. anophagefferens cells at a multiplicity of infection (MOI) of ~ 100 viral particles per A. anophagefferens cell (unless otherwise specified) to approach uniform infection (Gann et al., 2020a). To control for non-viral effects lysate may have on algal cells, lysate was sterilized through a 0.02- μ m Anotop 25 syringe filter (Whatman; Maidstone, United Kingdom) for all control infection cultures. Cell concentrations during infection were determined via flow cytometry (Chase et al., 2022). Following lysis of samples, aliquots were fixed using 1% glutaraldehyde for further enumeration of released viral particles. When infecting at lower MOIs, cell diameter measurements were determined via flow cytometry 23 h following infection before the

initiation of the light cycle. This allowed for measurements of cell size before cell lysis without the input of any additional light.

Transcriptome analyses of *Aureococcus* anophagefferens infection by AaV

We took advantage of an existing transcriptomics data set (Moniruzzaman et al., 2018) to query the progression of infection at the molecular level. Trimmed reads of infected and uninfected cultures of A. anophagefferens were mapped to the reference genome (GCF_000186865.1) using default parameters in CLC Genomics Workbench (v. 21.0.4) and read counts were analyzed for differential expression using DESeq2 (v. 1.42.0) in R 4.3.2 (Love et al., 2014). Control (uninfected) samples were compared to identify shifts in transcript abundance throughout the diel cycle. Control time points were divided into four periods based on when samples were collected during the original transcriptome. These samples were defined as early day, taken between 2 and 3 h after the initiation of the light cycle, late day, taken 8 h after the initiation of the light cycle, early night, taken approximately 30 min after the initiation of the dark cycle, and late night, taken 9 h after the initiation of the dark cycle. Individual genes with a \log_2 -fold change of at least 2 and a *p*-value of <0.05 for at least two of the four periods were defined as differentially expressed. The same parameters were applied to identify differentially expressed genes between control and infected treatments, though due to a limited number of identifiable genes at this level a log₂-fold change of >1.5 and a p-value <0.05 was used to identify other potentially altered expression levels. To identify other genes of interest that may be up or downregulated at a specific timepoint at a lower significance level, a \log_2 -fold change of 0.58 (a fold change of >1.5; p-value <0.05) was also examined. As a caveat, downregulation and upregulation will be used to equate proportional representation of mapped reads between treatments throughout this paper. Likewise, references to "differential expression" will be referred to in place of significantly altered transcript abundance levels.

To examine infection-driven inhibition of cell division, differentially expressed genes were filtered to only those associated with the cell cycle based on functional annotation in the *Kyoto Encyclopedia of Genes and Genomes* (KEGG Release 105.0) pathways map04110 (Cell cycle), map04111(Cell cycle – yeast), map04210 (Apoptosis), map04115 (P53 signaling pathway), and map04218 (Cellular senescence). Read abundance calculations for individual gene transcription trends and for incorporations into heatmaps were performed using the transcripts-per-million (TPM) method (Wagner et al., 2012). Heatmaps were constructed using *Heatmapper*. *ca* (Babicki et al., 2016) with genes clustered via single linkage clustering.

Determination of vertical transport rates

To assess the sinking rate of *A. anophagefferens* CCMP1984, cells in logarithmic growth were inoculated into a vertical settling column (Supplementary Figure S2; diameter=3.81 cm, height=25.4 cm, volume=290 mL) containing 225 mL ASP₁₂A and allowed to settle. After 2 h the bottom 50 mL of the column was drained through the

collection tube and agitated to homogenize the cells to a uniform concentration. This process was repeated for the remaining 200 mL of media. Cell concentrations and diameters were calculated via flow cytometry. To determine the sinking rate of infected cells, A. anophagefferens CCMP1984 was infected with AaV at an MOI of 100 either 2h (early infection) or 16h prior (late infection) to sinking rate assessment. Sinking velocity (Ψ) was calculated using the following formula:

$$\Psi = \frac{\beta s}{\beta t} * \frac{l}{T}$$

In which βs is total exported cells, βt is total cells in the column, l is distance traveled in meters, and T is time in hours (Bienfang, 1981; Mao et al., 2021).

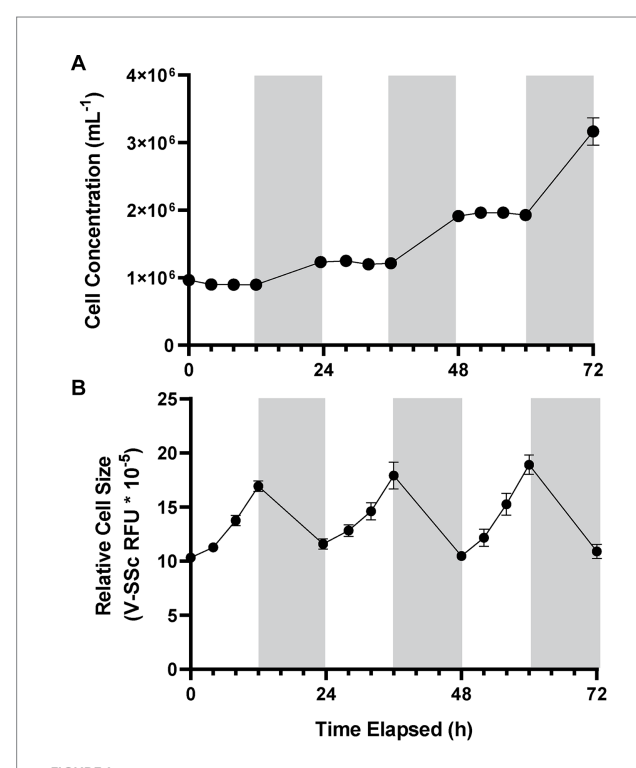


FIGURE 1 Cell concentration (A) and average cell diameter as measured via violet side-scatter (B) of A. anophagefferens CCMP1984 over the course of 72 h with samples taken every four hours during the light cycle. Periods of light are indicated in white, and periods of dark are indicated in gray (n = 5).

Statistical analyses

Population growth rate (r) was calculated using the following formula on cultures in exponential growth phase:

$$r = \ln\left(\frac{N_t}{N_0}\right) * \frac{1}{t}$$

Where *t* is time in days, N_t is the cell concentration at the time in days, and N_0 is the initial cell concentration.

Statistics were performed using Prism 9.1.0. Differences between population growth rates, cell sizes, and sinking rates were determined using a one-way ANOVA followed by Tukey's post hoc testing using a standard significance level of p < 0.05 unless otherwise noted. Correlation coefficients were determined using a simple linear regression. Non-metric multidimensional scaling (nMDS) and hierarchical clustering analysis of host transcriptional shifts in the uninfected reference transcriptome was performed in PRIMER v7.0 (Clarke, 2015) using a Bray–Curtis dissimilarity matrix.

Results

Diel partitioning of cellular growth and division

A. anophagefferens CCMP1984 cultures grown under a 12:12 light:dark cycle were observed every 4h during the light period to determine cell concentration and relative fluorescence measurements throughout the light cycle. During light periods, A. anophagefferens CCMP1984 cell densities were generally constant (Figure 1A). However, after the dark period, cell abundance increased, consistent with a diel association with cellular division. V-SSc relative fluorescence indicated a similar pattern between the light and the dark cycle, with average cell diameter (Supplementary Figure S2) and V-SSc fluorescence (Figure 1B) increasing throughout the day and reducing during the night. Population-wide increases in cell size were not linear, with the rate of cell diameter growth increasing along with the length of exposure to light. While other strains of A. anophagefferens differed in specific population growth rate and percent change in cell size over light and dark periods, all strains we tested followed the pattern of division in the dark, impeded division during the day, and cyclical cell-size changes (Table 1). A significant increase in cell density occurred within eight hours of the dark period for CCMP1984 (p = 0.024) and within 12h of the dark period for CCMP1850 (p = 0.051) (Supplementary Figure S3).

TABLE 1 Mean population growth rate and changes in cell diameter through either light or dark periods of three different strains of A. anophagefferens.

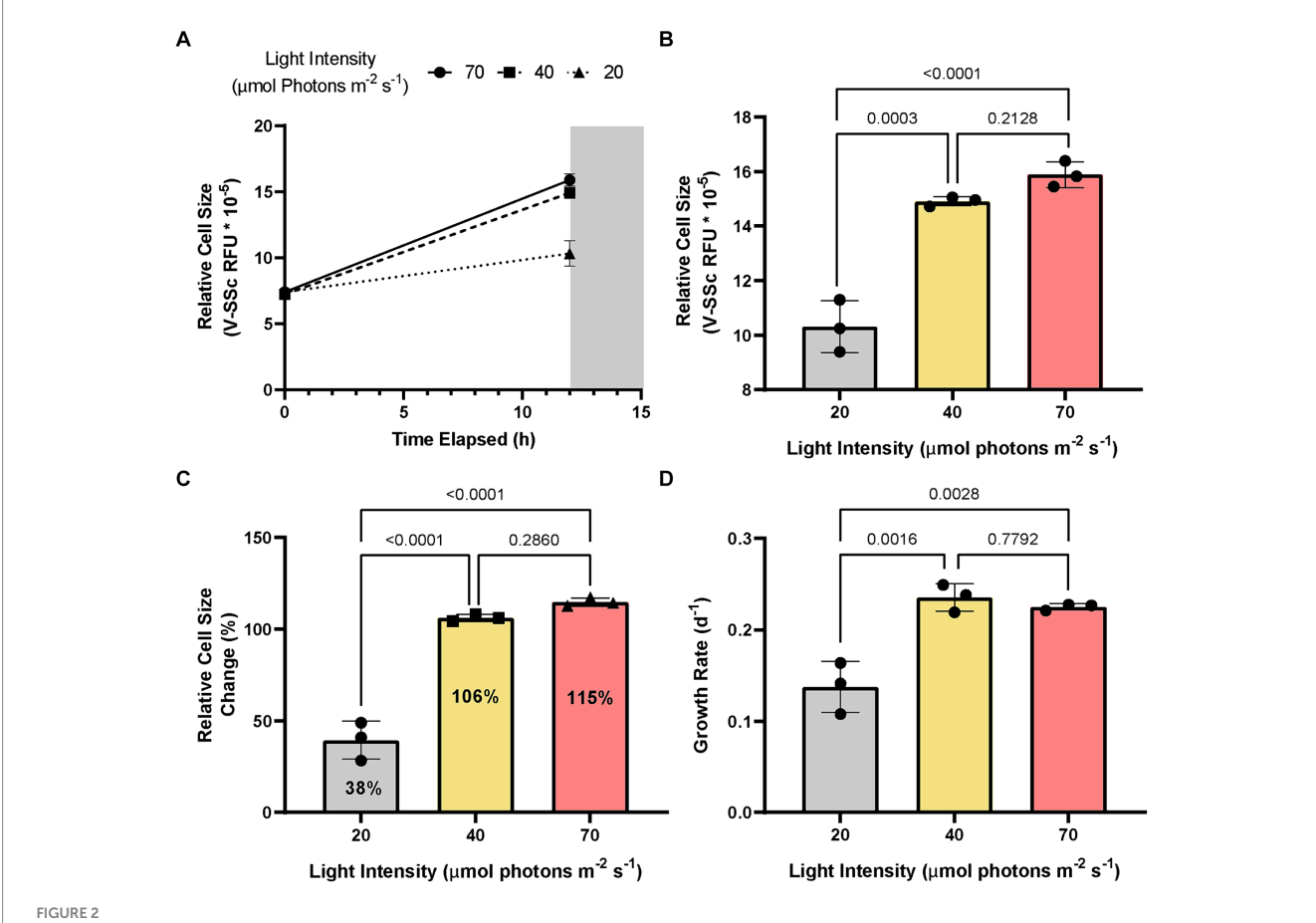
	CCMP1850	CCMP1984	CCMP1707
Total growth rate (D ⁻¹)	0.373 (± 0.06)	0.386 (± 0.05)	0.251 (± 0.04)
Day growth rate (D ⁻¹)	0.089 (± 0.07)	0.023 (± 0.05)	0.026 (± 0.05)
Night growth rate (D ⁻¹)	0.657 (± 0.13)	0.749 (± 0.12)	0.475 (± 0.06)
Day change in cell diameter (%)	23.44 (± 2.58)	35.54 (± 2.79)	15.15 (± 1.36)
Night change in cell diameter (%)	-26.25 (± 3.03)	-30.35 (± 3.68)	-18.96 (± 1.25)

Standard deviation is denoted in parentheses.

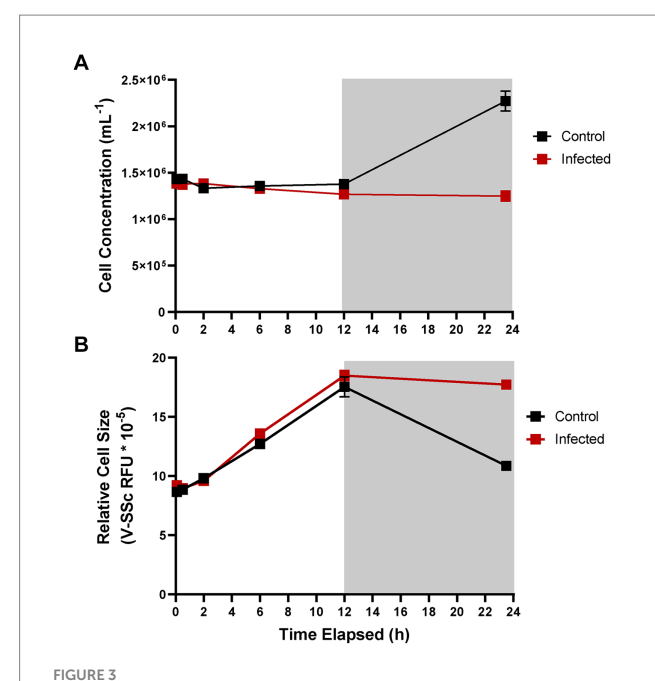
Given A. anophagefferens CCMP1984 has been maintained in our laboratory for an extended period (over 10 years) and thus these light settings may have selected for specific growth patterns, circadian rhythms could not be ruled out as a factor in diel-associated cellular growth and cell division. To test this possibility, A. anophagefferens CCMP1984 cultures were exposed to reduced light levels. While no discernable growth differences were detected between medium and high light levels (40 and 70 $\mu mols$ photons $m^{-2}\ s^{-1},$ respectively; p-value = 0.213), cell diameters in cultures maintained at 20 μmols photons m⁻² s⁻¹ had significantly (p-value <0.0001) reduced diameters (~ 2.4 μm), as compared to high light treatments (2.9 μm) after 12 h of light exposure. Cells in low light cultures increased in diameter by 38.3%, while full irradiance cultures increased in diameter by 114.8% (Figures 2A-C). Population growth was also significantly impeded in low light cultures over 72 h (Figure 2D). Entraining cultures on a 12:12 light:dark cycle only to leave the lights off after 12 h of darkness showed that A. anophagefferens did not in these instances display any characteristics of a free-running clock (Supplementary Figure S4). Furthermore, A. anophagefferens had population growth rates of approximately zero or lower when exposed to 24 h light or 24 h dark (Supplementary Table S1). In 24 h light, cells continuously increased in size over the course of 48 h, while cells continuously decreased in size in 24 h darkness (Supplementary Table S1). While increasing the length of the light period did lead to continued increases in cell size, longer light periods did not have much effect on net population growth rate.

Infected cells increase in diameter while division is inhibited

A. anophagefferens CCMP1984 was infected with AaV to observe the effects of viral infection on the diel growth cycle. During the first 12 h of infection, (during the light cycle) no differences were observed between infected and control samples treated with filtered lysate (Figure 3). However, during the night cycle, infected cultures did not divide and stayed at the same cell concentration (Figure 3A) and cell diameter observed at the termination of the light cycle (Figure 3B). Following the first 24 h, average cell diameter increased again, up to an additional 21% increase from the first light cycle (Figure 4C). It is unclear if the cells that continued to increase in size were the same group of infected cells or were instead previously uninfected cells that continued to skew the average size higher as they continued to grow. To determine whether size shifts between infected and uninfected cells



Physiological parameters for cultures kept at three different irradiance levels (high: red, ~70 μ mol m⁻² s⁻¹; medium: yellow, ~40 μ mol m⁻² s⁻¹; low: grey, ~20 μ mol m⁻² s⁻¹). (A) Change in average *A. anophagefferens* CCMP1984 cell diameter as measured via violet side-scatter over the course of a single 12-h light period. (B) Final average cell diameter at the termination of the light period. (C) Proportional change in cell size over the course of the light cycle. (D) Population growth rate of *A. anophagefferens* CCMP1984 over the course of 72 h under the three irradiance levels. *p* values are represented above separate irradiance levels compared via two-way ANOVA and post-hoc multiple comparisons adjusted with Tukey's HSD (n=3).



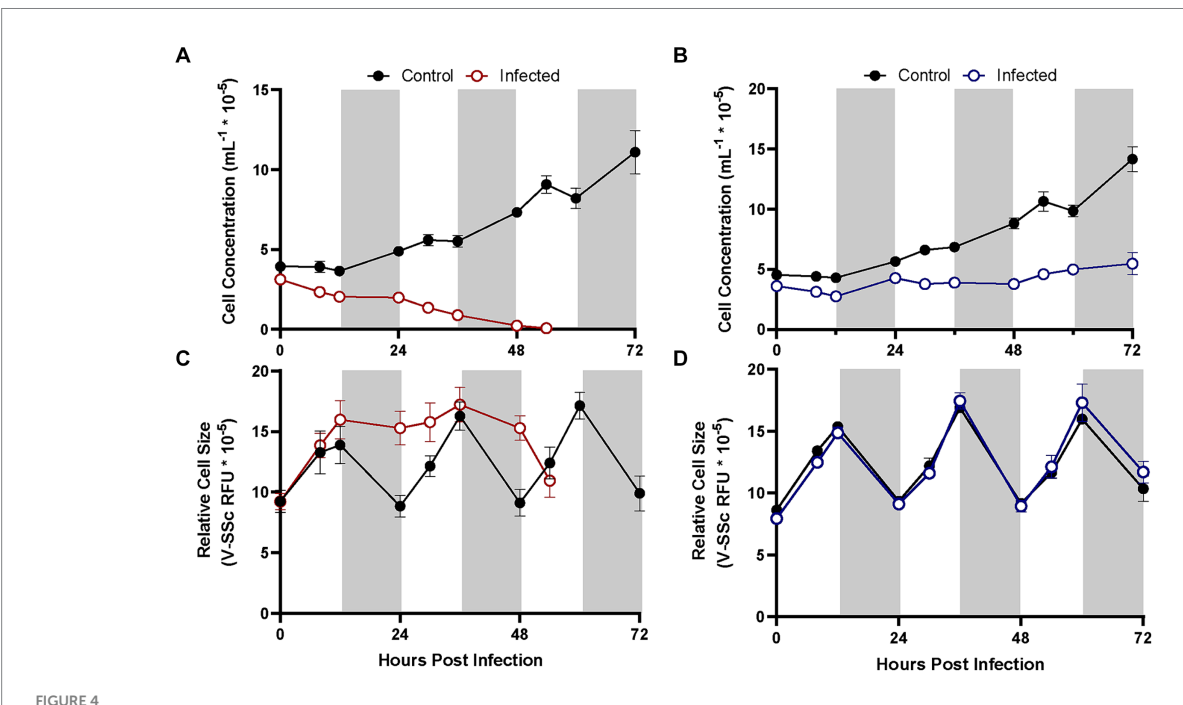
Cell concentration (A) and average cell diameter as measured via violet side-scatter (B) of A. anophagefferens CCMP1984 over the course of 24 h in the presence of AaV. Samples treated with viral lysate are indicated in red and control samples are indicated in black. Light periods are indicated by a white background while dark periods are indicated with a grey background (n = 3). Infected samples were treated with pre-enumerated lysate at an MOI of 100 viral particles per cell.

were evident in a single culture, size was measured at lower MOIs approximately 23 h following infection. A higher MOI led to an increased average diameter of infected cultures following the night cycle, with cultures infected at an MOI of 100 displaying a 30% increase in average V-SSc as compared to those infected at an MOI of 10 (Table 2; Supplementary Figure S5). A negative correlation $(R^2 = 0.9427, slope = -0.372)$ between MOI and percent similarity in size of infected cultures to control cultures was found (Supplementary Figure S6A).

A. anophagefferens strain CCMP1850 which displays a resistant phenotype to viral infection by AaV was tested for its physiological response to viral exposure over the course of several days. Additional increases in cell diameter following the initial 24-h period in infected strains was evident in CCMP1984, before average cell diameter diminished coinciding with the total lysis of the culture around 48 h (Figure 4). CCMP1850 also appeared to be inhibited in cell division (Figure 4B) but maintained normal cell size cycling throughout the light: dark period as compared to uninfected cells (Figure 4D).

Separate cell cycle transcriptomic activity between day and night

We returned to a transcriptome from a previous infection study (Moniruzzaman et al., 2018) to identify cell division genes differentially expressed between the light and dark periods. Samples were subdivided into four categories: the early day (n = 9, 2 to 3 h into the light period), late day (n = 3, 8 h into the light period), early night



Growth of different A. A anophagefferens strains CCMP1984 (A,C) and CCMP1850 (B,D) in the presence and absence of viral lysate over the course of 72 h. Cell concentrations (A,B) and relative cell size (C,D) are denoted. Light periods are indicated by white backgrounds while dark periods are indicated by gray backgrounds. Black lines represent uninfected cultures, solid-colored lines represent cultures infected at the initiation of the light cycle (n = 3). Infected samples were treated with pre-enumerated lysate at an MOI of 100 viral particles per cell.

TABLE 2 Growth and division characteristics of A. a	anonhagefferens CCMP1984 23 h followin	a viral infection with AaV at variable MOIs

	Control	MOI 10	MOI 50	MOI 100
Growth rate (D ⁻¹)	0.535 (± 0.16)	0.191 (± 0.20)	0.100 (± 0.17)	-0.379 (± 0.16)
Cell size after night cycle (V-SSc * 10 ⁻⁵)	7.352 (± 0.091)	7.981 (± 0.121)	9.545 (± 0.569)	10.410 (± 0.639)
Percent decrease in cell size (%)	38.87 (± 4.19)	29.41 (± 4.47)	22.13 (± 2.08)	20.48 (± 1.52)

Cell size following the night cycle was recorded prior to the initiation of light cycle. Percent change in cell size was determined based on the peak cell size at the initiation of the dark cycle and the final size at the end of the dark cycle. Standard deviation is denoted in parentheses.

 $(n=3, \sim 30\,\mathrm{min}$ into the dark period), and late night $(n=3, 9\,\mathrm{h}$ into the dark period). Cluster analyses revealed an almost cyclical relationship among uninfected samples with similarity between categories strongest for neighboring groups (e.g., late day was most like early day and early night) (Supplementary Figure S7). Gene set enrichment analysis revealed enrichment of cell cycle-associated transcripts between time points, most evidently when comparing the early night time point to all other time points (normalized enrichment score=1.80, p-value=0.0) (Supplementary Table S2). Although we will focus on homologs of cell cycle-associated genes, in total 1,823 genes were identified as differentially expressed between at least two of the time periods analyzed under our highly conservative parameters (Supplementary Table S3).

A clear partition in cell cycle gene read counts throughout different stages of the day was evident (Figure 5). Periods that differed most notably from one another were the early day/early night (22 differentially expressed genes; Supplementary Figure S8) and the late day/late night (13 differentially expressed genes; Supplementary Figure S9). Cohesin subunit homologs (scc1, scc2, scc3, smc1, and smc3) were differentially expressed between early morning and early night (Figure 5; Supplementary Figure S8) with a consistent drop off in expression during the late night and markedly low expression throughout the day (Figure 5; Supplementary Figure S9). Condensin subunit-like genes smc4 and ycs4 were overexpressed during the latenight timepoint as compared to the day, with steady down regulation of ycs4 in the early night (Figure 5; Supplementary Figures S8, S9).

Regarding cyclin associated homologs and their expression throughout the cell cycle, ccnb2 (Cyclin B) was expressed significantly more at night as compared to the day (\log_2 fold change=2.47, p < 0.001), though one homolog (ccnb2i; 12473) was under expressed in the early night as compared to the morning. A cdc20 and a cdk1 homolog were expressed late at night, but not earlier. Cdc45 was also expressed early in the night and not present late at night.

A homolog for tumor (i.e., cell division) suppressor gene p53 is not encoded by *A. anophagefferens*. Still, certain homologs of genes associated with p53 do display changes in expression. In the early day *mdm2* was highly expressed, while it was downregulated in the early night. It was also highly expressed late at night and barely expressed mid-day. A homolog of tumor suppressor *rb1* was differentially expressed in the late day/early night period from the morning. Cell cycle regulation genes *tp53i3* (tumor protein p53 inducible protein 3), *hrad1* (Rad1 checkpoint protein homolog), *atm* (serine/threonine kinase), *erk* (extracellular signal-regulated kinase), and *rrm2* (ribonucleoside reductase regulatory subunit M2), many of which are expressed downstream of p53, also followed this pattern (Figure 5).

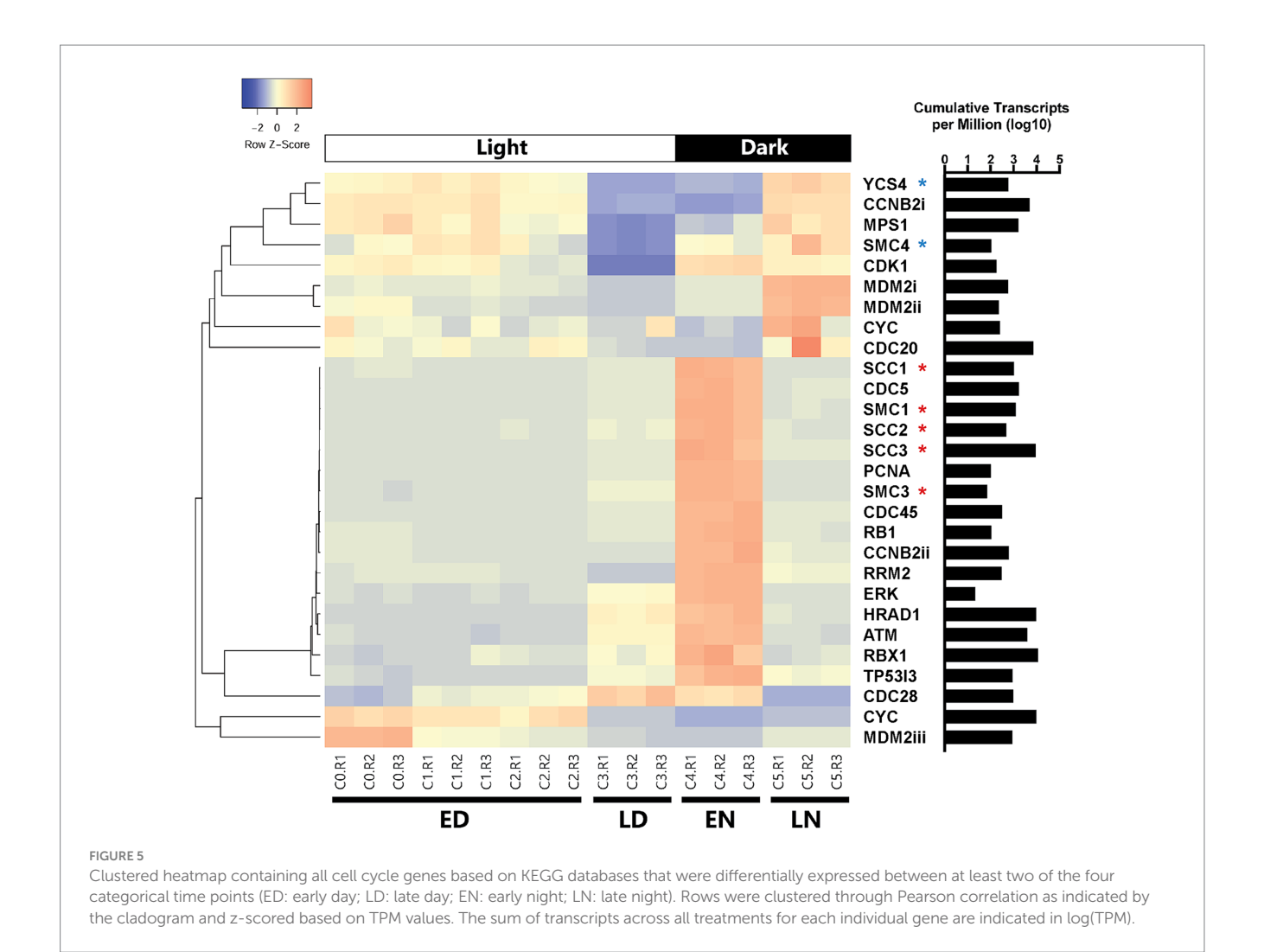
DNA damage and p53-associated genes respond to AaV infection

Given cell division appears inhibited when A. anophagefferens is infected with AaV, we sought to identify associated genes that might be targeted by the virus for regulation. When comparing the infection transcriptome to the control, only 11 cell cycle associated genes were identified at a \log_2 -fold change of ≥ 1.5 (Table 3). While most of these genes were in the late night time point of the infection cycle, three genes were identified 12 h following infection (early night) and one at the 6 h mark (late day). Interestingly, all three genes identified at the 12 h timepoint were homologs of the mdm2 gene, two of which were down-regulated in the infected samples with the other highly up-regulated. While all these transcripts increased in abundance as the night continued, their role in infected samples in the early night may also be relevant.

At the 21-h timepoint, seven cell cycle genes were differentially expressed between control and infected samples, including four SMC-like genes. Two cohesin-associated genes were up-regulated (*smc1* and *smc3*), one condensin-associated gene was up-regulated with the other down-regulated (*smc2* and *smc4*, respectively) (Supplementary Figure S10). The cell cycle regulatory genes *skp1* and *pcna* were also upregulated at this time point, while another regulator of the cell cycle, *myt1/wee1* was downregulated.

Using a less conservative method for defining differential expression [i.e., the 1.5-fold change described in Moniruzzaman et al. (2018)] an additional 64 cell cycle genes were differentially expressed between all infected and control samples (Figure 6; Supplementary Table S4). Among these genes, seven were consistently upregulated in infected samples, 19 were consistently downregulated, and five alternated between upregulated and downregulated. Multiple inhibitors of cell cycle regulation genes (*myt1*/wee1) were consistently upregulated, including a protein arginine methyltransferase (*prmt5*) and *rbx1*. Also upregulated was a ubiquitin-protein lyase homolog (*siah1*).

Of the consistently down-regulated genes, many are associated with DNA replication and checkpoints for DNA damage repair. Regarding initiation of replication, two mini-chromosome maintenance (MCM) subunits and one origin recognition complex (ORC) subunit were downregulated in infected samples. Likewise, downregulated DNA damage response genes include *rrm2*, *prkdc*, *ddb2*, and *myt1/wee1* (Supplementary Figure S10). Condensin and separase (*esp1*) transcripts decreased in abundance as well. Outside of genes associated with DNA replication and repair are various other downstream effectors of the conventional p53 pathway. Negative feedback regulators including the previously mentioned three *mdm2*



homologs and the ppm1d protein phosphatase were downregulated throughout the infection cycle.

In addition to shifts in transcript abundance across all time points, genes differentially expressed at single time points may provide insight into how viral infection impacts the cell cycle of *A. anophagefferens*. For instance, while several condensin-associated genes were downregulated at the 12 h time point, they became upregulated at the 21 h time point. The *rb1* homolog was also upregulated at the 21 h time point. Interestingly, while a cyclin B homolog was downregulated at the 21 h time point, cyclin D and cyclin H were upregulated at 12 and 21 hours post infection, respectively (Supplementary Table S4). Cyclin-dependent kinases also acted contrarily, with some (*cdc28*, *cdc6*, *cdc5*, *cdc15* and *cdk1*) downregulated at certain time points and other (*cdc7* and *cdk1*) upregulated (Supplementary Table S4).

Infection alters host cell sinking rate

To assess biophysical consequences of diel shifts in cell size/composition in the presence and absence of AaV, sinking rates of A. anophagefferens were measured. A. anophagefferens sinks in the water column in vitro and accumulates at the bottom of the given culture flask. The sinking velocity of uninfected A. anophagefferens cells varied

independently of time of day or cell size (Supplementary Figure S11). Within 2 h of infection of *A. anophagefferens* by AaV, the alga sinking rate increased compared to control (uninfected) cells (Figure 7A). A similar trend was noted 16h after infection, showing cells in the early and late stages of the virocell state were exported from the water column at the same rate (Figure 7A). When comparing cell diameter or volume for uninfected cells at the bottom of the settling column to cells at the top, there were no significant differences (Figures 7B,C).

Discussion

In the past, studies of marine algal growth patterns have generally been conducted with daily sampling at consistent time points (relative to light: dark cycles) (Tang, 2003; Shirai et al., 2008; Perrin et al., 2016; Gann et al., 2020b, 2022). While this method increases comparability over long-term sampling schemes, it excludes physiological changes that occur in response to prolonged exposure to light or the absence of light. Thus, other time points (e.g., 6 daylight hours, 12 daylight hours, etc.) likely need to be considered as they potentially offer other physiological states. Furthermore, studies that have focused on hourly changes in algal growth dynamics often have not considered the growth cycle, physiology, and metabolism of virocells which may

TABLE 3 Aureococcus anophagefferens cell cycle-associated genes that are differentially expressed (p-value <0.05, log₂fold change >1.5 or < -1.5) at either the 6 h, 12 h, or 21 h timepoints between infected and uninfected samples.

Gene ID #	Gene name	Time	Direction	Fold change (log₂)	Notes
32157	cdc15	6	Down	-1.51	Protein kinase; cell division control protein
12504	mdm2	12	Up	2.79	E3 ubiquitin-protein ligase; p53 regulation
24297	mdm2	12	Down	-1.72	E3 ubiquitin-protein ligase; p53 regulation
3154	mdm2	12	Down	-1.51	E3 ubiquitin-protein ligase; p53 regulation
36910	smc2	21	Up	1.84	Structural maintenance of chromosome; Condensin subunit
58667	skp1	21	Up	1.82	S-phase kinase-associated protein 1; Myt1 regulator
70503	smc1	21	Up	1.81	Structural maintenance of chromosome; Cohesin subunit
70163	рспа	21	Up	1.77	Proliferating cell nuclear antigen
72635	smc3	21	Up	1.55	Structural maintenance of chromosome; Cohesin subunit
72516	myt1	21	Down	-1.75	Mitosis inhibitor protein kinase
72033	smc4	21	Down	-1.5	Structural maintenance of chromosome; Condensin subunit

make up a significant portion of the natural community (Brussaard et al., 1996; Vincent et al., 2021). Indeed at least some algal viruses rely on light during infection (Derelle et al., 2018; Gann et al., 2020a) with certain giant viruses even encoding rhodopsins (Needham et al., 2019). Collectively this implicates the diel cycle as a potential modulator of virus activity in phototrophs. We examined physiological shifts of infected and uninfected *A. anophagefferens* in the context of diel periodicity. We also explored transcriptomic data to understand shifts in transcript abundance in infected and uninfected cells.

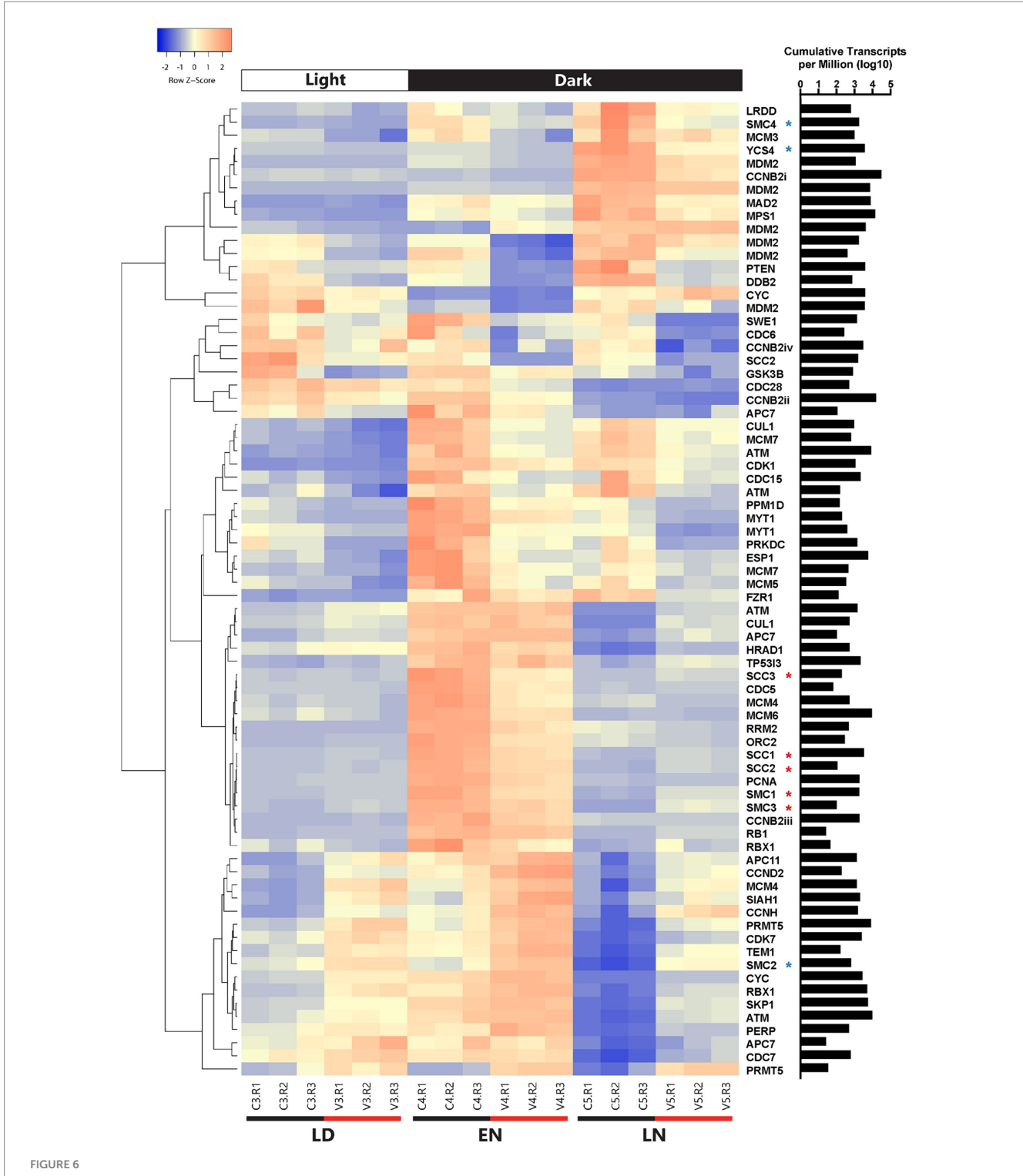
Cellular and population growth of Aureococcus anophagefferens is constrained by the diel cycle

A. anophagefferens cell diameter gradually increased during the light period, with cell division (i.e., size reduction and cell density increase) almost exclusively occurring during the dark period. While this separation of growth and division has been observed in phytoplankton, rarely has the distinction been so clear, as cellular growth is often seen during both dark and light periods (Harding et al., 1981; Goto and Johnson, 1995; Jacobsen and Veldhuis, 2005; Moulager et al., 2007). Moreover, we observed no change in cell concentrations during the light period, with occasional (yet statistically insignificant) decreases in cell count when the light period is increased (Supplementary Table S1). Attempts to disrupt the diel cycle by extension of light or dark periods or incident light reduction revealed that the growth periods observed under normal conditions were primarily associated with the diel cycle, and not a result of circadian rhythms. A. anophagefferens does encode a homolog of an animal-like cryptochrome containing a photolyase domain, meaning circadian responses to light are not necessarily absent in this system (Petersen et al., 2021). While circadian control of the cell cycle has only been studied in a few model species (Chlamydomonas reinhardtii, Ostreococcus tauri, Phaeodactylum tricornutum), it is possible that specific expression levels of cell cycle-associated genes are constrained to a circadian clock in A. anophagefferens, without strict constraint of carbon fixation and cell growth-associated genes (Coesel et al., 2009; Heijde et al., 2010; Beel et al., 2012; Petersen et al., 2021). This necessitates further analyses of transcriptomic and proteomic profiles of *A. anophagefferens* under a free-running clock to draw any further conclusions.

Pelagophytes like *A. anophagefferens* exist in open oceans at the deep chlorophyll maximum, spatially deeper than cyanobacteria and dinoflagellates (Latasa et al., 2017). Given a preference for decreased light and increased nutrient availability, it is possible that these cells are highly susceptible to photooxidative stress and DNA damage when unshaded (Latasa et al., 2017). If light stresses are a factor, cells may benefit from cell division and DNA synthesis occurring during dark periods. G1 to S phase likely requires a DNA damage checkpoint to be met, though the genes regulating this transition are not well defined in *A. anophagefferens* (Hlavová et al., 2011). It is possible that to proceed to the downstream transcriptional effects of the cell cycle, a photoreceptor-like trigger must first be deactivated, akin to the red/far-red phytochrome receptor in plants (Mawphlang and Kharshiing, 2017). This is supported by our work showing that *A. anophagefferens* cannot grow in 24-h light.

Virocells display arrested division phenotypes but continue to respond to light exposure

Infection of A. anophagefferens by AaV inhibited cell division during the dark period of the diel cycle. The virocells maintained the same size overnight, as opposed to the uninfected cells which decreased in average diameter in parallel with division. Virocells also did not divide (Figure 3). One explanation for the inability to divide may be diversion of host energy away from the cell cycle to stress response mechanisms, as has been observed in response to other stressors (Terhorst et al., 2023). However, large DNA viruses, as well as retro and RNA viruses, have been noted for their ability to disrupt the cell cycle by blocking entry into S phase or causing cells to accumulate in G2 phase (Emmett et al., 2005). This active disruption may benefit viral propagation as increased volume of the cell and reduced host usage of cell cycle resources may drive increased virion production (Flemington, 2001). It is possible that the cells were unable to enter mitosis either through degradation of the host genome by viral endonucleases or an increase in the density of



Clustered heatmap containing all cell cycle genes that were differentially expressed between infected and uninfected *A. anophagefferens* at one or more timepoints (LD: late day; EN: early night; LN: late night). Early morning timepoints were not included due to high variability in transcript abundance among infected samples at this period. Infected samples are indicated by a V and control samples are indicated by a C. Rows were clustered through Pearson correlation as indicated by the cladogram and z-scored based on TPM values. The sum of transcripts across all treatments for each individual gene are indicated in log(TPM).

early-stage viral particles. Likewise, virus-induced physiological changes to structures important for cell cycle progression, like repurposing the nucleolus (Emmett et al., 2005; Matthews et al., 2011) and reorganization of host microtubules (Naghavi and Walsh,

2017) could feasibly prevent the cell cycle from progressing. However, viral particle formation and the degradation of most organelles does not occur until later in the infection cycle. This leads to the possibility that transcription under viral infection prevents the cell cycle from

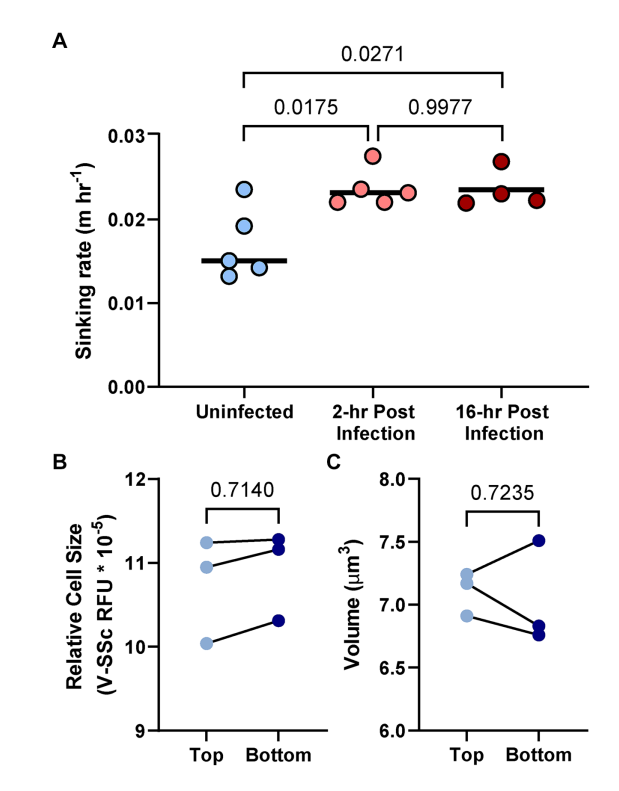


FIGURE 7
Sinking rate of A. anophagefferens CCMP1984 cells as it relates to the length of infection (A), relative fluorescence as a proxy for cell diameter (B), and volume as determined via the FlowCam (C) of CCMP1984 in the top portion and bottom portion of the sinking column after incubation. Lines connecting data points signify samples taken from the same sinking column. Numerical p-values calculated via one-way ANOVA (A) and paired t-test (B,C) are denoted

progressing and locks the infected cells into a prolonged G2 phase before the cell can enter mitosis. This is notably not the only outcome of virus-host interaction, as infecting the partially resistant CCMP1850 with AaV reveals inhibition of division but consistent cycling of cell size (Gobler et al., 2007). This may imply that whatever stress viral presence places on this strain, it is unrelated to diel cycling and the cell cycle.

Another element of the infection dynamics of A. anophagefferens and AaV is the similar growth during the light cycle between infected and uninfected samples. As previous studies have shown, light is an important constraint on the burst size of AaV (Gann et al., 2020a). Combined with the fact that viral production approaches zero under very low light conditions ($\leq 5 \,\mu \text{mol photons m}^{-2} \,\text{s}^{-1}$) (Gann et al., 2020a), successful infection of a host may require a prolonged irradiance period. While transcription of viral genes begins within the first five minutes of infection, the cellular growth during light periods remains the same, meaning this portion of the growth cycle is perhaps relevant to the virus's propagation. While we may define this period as nutritional stockpiling by an uninfected host to prepare for DNA synthesis and cell division, in the case of viral infection the same stockpiling must occur, only to be used in production of viral particles (Gann et al., 2020b). In considering what metabolic processes the virus alters for its own benefit, we also must consider which processes are left unaltered and how these too may serve a purpose in viral infection.

Aureococcus anophagefferens' cell cycle is transcriptionally constrained to diel effects

Analysis of the viral infection transcriptome revealed that cell cycle arrest and regulation genes were changed during viral infection, but also that transcription of many cell cycle-associated genes in uninfected cells is constrained to a diel cycle. Notably, a significant contingent of cell cycle genes are enriched at the early night time point, implicating a shift in gene expression following the termination of the light cycle (Supplementary Table S2). One of the most consistent observations of diel-driven differential expression within this dataset was the expression of cohesin and condensin genes. The cohesin complex, which binds sister chromatids together following DNA replication and prior to anaphase, acts as an important intermediate complex before sister chromatids are segregated to opposite ends of the cell (Peters et al., 2008). The condensin complex begins functioning typically after the nuclear envelope has broken down from prophase to anaphase (Hirano, 2012; Leonard et al., 2015). Further research has shown that in C. reinhardtii, condensin subunits are likely involved in proper formation of the mitotic spindle (Breker et al., 2018). The expression patterns of these subunits in A. anophagefferens, cohesin homologs upregulated in the early night and condensin homologs upregulated in the late night, suggest that cells were progressing through mitosis at these time points. Thus, DNA replication likely occurred either soon before or after the dark period began. Likewise, we have shown that cell division primarily occurs after 6-7h in the dark (Supplementary Figure S3), meaning condensin should be heavily expressed at this time point (Skibbens, 2019).

Further evidence for the temporal partitioning of cell cycle pathway genes is shown by the expression pattern of pcna (Liu et al., 2005). In the red alga Cyanidioschyzon merolae, pcna was used as a marker of cell cycle progression and peaked in fluorescence mid S-phase, before dissipating throughout the remainder of the cell cycle (Sumiya et al., 2014). A similar expression was observed in the A. anophagefferens control transcriptomic dataset, with the pcna homolog exclusively peaking in expression in the early night. This indicates DNA synthesis may occur around the transition from light to dark. Along with pcna, several other A. anophagefferens genes including cyclin B (ccnb2ii), cdc45 [which has been tied to replication fork initiation (Sanchez-Pulido and Ponting, 2011)], cdc5, five cohesin subunits, and the DNA damage repair gene rrm2 show this pattern (Figure 5). We hypothesize that these genes are largely associated with DNA synthesis. Several genes expressed heavily in the early night are also detected at increased levels in the late day (tp53i3, hrad1, atm, and erk). Such genes could be attributed to acting as a catalyst for DNA damage repair and preventing cellular division with damaged or incompletely replicated DNA. Likewise, a close homolog to the yeast gene cdc28, which is active late in G1 phase (Mendenhall and Hodge, 1998), was upregulated in the early hours of the night, as well as mid-day, identifying a possible early trigger to encourage DNA synthesis in A. anophagefferens. This gene is notably not expressed in the late night, signaling that many cells may have progressed past the early stages of the cell cycle.

Among the *A. anophagefferens* genes expressed differentially in the late night were the p53 inhibiting *mdm2* homologs, *cdc20*, monopolar spindle 1 kinase (*mps1*), and two condensin subunits, of which *A. anophagefferens* only encodes three (Figure 5). Based on the presence of genes like *cdc20*, *mdm2* and *mps1* which actively either drive or regulate mitotic cell division (Mendoza et al., 2014; Pecani et al., 2022), it seems evident that the cells at the late time point were actively in the process of mitosis. Their abundance in these contexts indicates cell division may be heavily down-regulated late in the day but encouraged after several hours in the night cycle. However, due to the nature of this study, the turnover of RNA throughout the day is uncertain, and increases in transcript counts may be a result of accumulation throughout the entire day.

AaV infection drives transcriptional shifts in cell cycle regulation

Viral infection of A. anophagefferens revealed heavy regulation of genes associated with DNA replication. Several cohesin subunits and the pcna gene were upregulated late in the infection cycle (late night) after their transcript levels had decreased in the control samples (Figure 6). These genes may be utilized in replication of the viral genome, which would justify such an elevated expression level. Host cohesin genes have specifically been identified as important factors in the infection cycle for other DNA viruses (Li et al., 2021). Notably, many genes associated with cell cycle arrest based on DNA damage have altered expression levels during viral infection (Figure 8). Three homologs of myt1/wee1, which can induce cell cycle delay (Détain et al., 2021), were downregulated in A. anophagefferens under infecting conditions, one of which was downregulated at all three latter time points. WEE1 is typically considered a tumor suppressing protein and is often involved in the prevention of mitosis when DNA is damaged by way of phosphorylating CDK1 (Hlavová et al., 2011; Luserna et al., 2020). In accordance with this downshift in expression, four negative regulators of wee1 (cul1, skp1, rbx1, and prmt5) (Watanabe et al., 2004; Jia et al., 2011; Beketova et al., 2022; Zhang et al., 2023), were frequently upregulated during infection while three more genes associated with suppressing the cell cycle due to DNA damage (rrm2, prkdc, and ddb2) were downregulated (Chen L. et al., 2021; Chen S. et al., 2021; Zuo et al., 2024). DNA damage repair has previously been found to limit the cytotoxicity of adenoviruses (Connell et al., 2011), thus downregulation of these genes could promote untethered viral genome replication. To further associate the DNA damage with viral genome replication, ubiquitination of PCNA by certain checkpoint proteins may lead to stalling of replication (Moldovan et al., 2007), thus it is possible an upregulation of this gene as well as a down-regulation of damage associated genes would allow for viral DNA synthesis to proceed. The role of these genes has gone understudied in algae and the *Nucleocytoviricota* alike and further analysis is warranted.

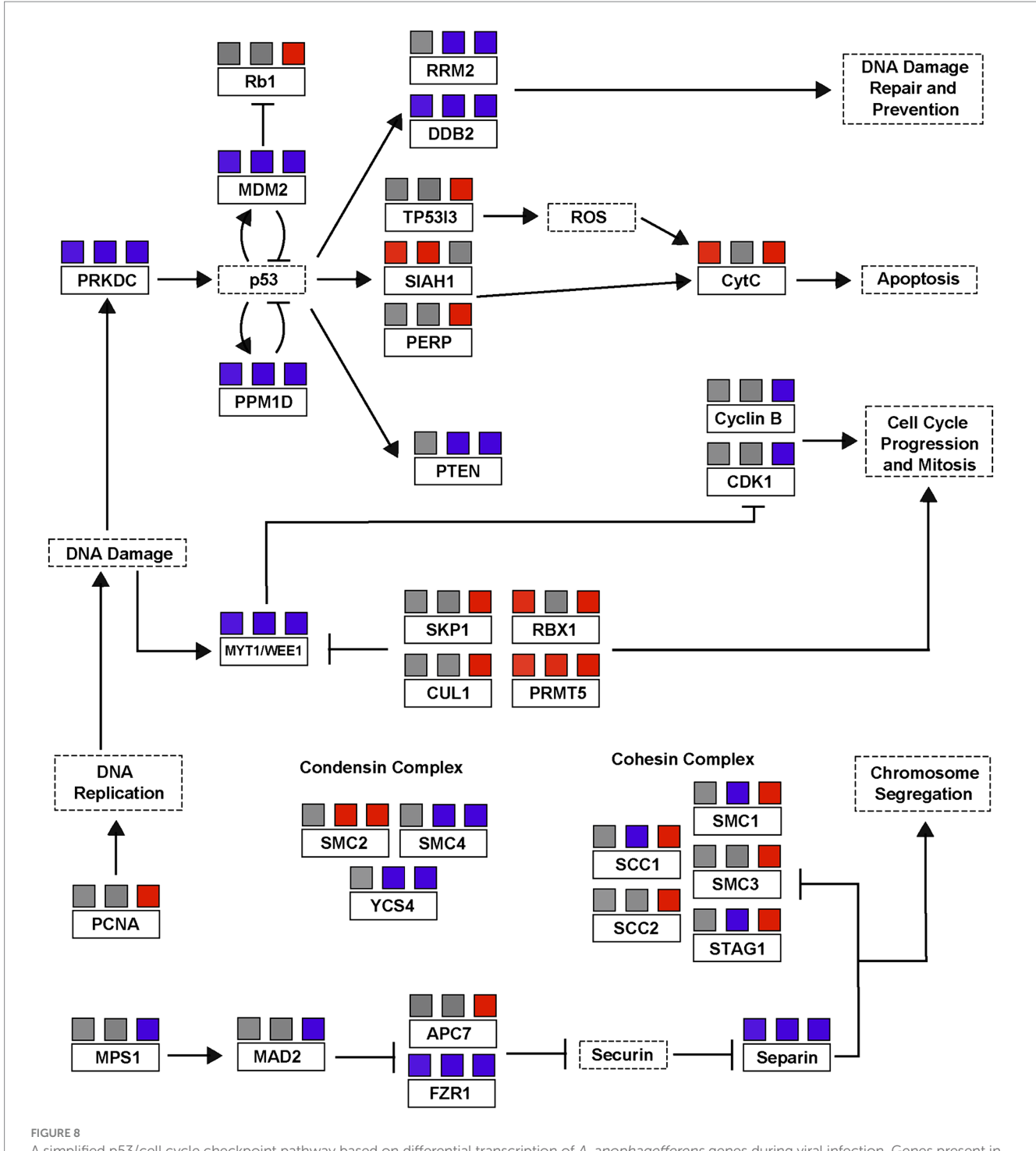
From this concept there arises a conflicting dichotomy in the viral transcriptome in which genes that both lead to and prevent cell cycle arrest are regulated. While these DNA damage checkpoint genes may be downregulated, p53 inhibitors, which would naturally promote the cell cycle, are downregulated as well (Figure 8). We see a very complex expression pattern in which some homologs of the downstream effectors of p53 like the apoptotic pathway, *siah1* (Frew et al., 2002), and *rb1* are promoted under viral expression, while others that relate back to DNA damage control which might halt the cell cycle during

S-phase are blocked in expression. Other DNA viruses, including papilloma viruses and adenoviruses, encode genes which can induce apoptosis to aid in viral dissemination (Gupta et al., 2015). Another perspective is that certain promoters of cell cycle progression are not altered by viral infection. While a total of 175 A. anophagefferens genes were functionally categorized as cell cycle genes, only 74 of them appeared in our differentially expressed dataset, meaning over 60% were statistically unchanged by viral infection. For example, A. anophagefferens encodes for 10 anaphase promoting complex gene homologs, only one subunit was downregulated at one time point. While this does not confirm that these processes were not at all affected by the invading virus, it does suggest that continued activation of some of these pathways has at the very least a net neutral effect on viral particle production. A highly specialized virus must be able to streamline the infection process, and the host processes that are neutral, beneficial, or essential must remain active while anything deleterious be targeted for downregulation. For this reason, we believe that if the virus prevents the host cell from entering mitosis, the natural progression of the cell cycle may be important for the culmination of the infection cycle.

Though these possibilities are intriguing, our interpretations are limited by the lack of a complete cell cycle model in *A. anophagefferens*. Not only are most of the genes described herein attributed to putative functions through sequence homology, but many common genes also appear to be completely missing. For example, there are zero homologs to conventional CDK inhibitors encoded in any sequenced *A. anophagefferens* genome. Likewise, though we reference the p53-associated pathway for growth suppression often, there is no known homolog for p53 encoded by *A. anophagefferens* or any other plant or algal lineage. However, with such a robust representation of associated genes, including the direct downstream gene of *tp53i3* and the high abundance of *mdm2*-like p53 regulators, the presence of a functional p53 equivalent in *A. anophagefferens*, as well as other algae, is likely (Nedelcu, 2006).

Export from the water column is enhanced by viral infection

Settling rate assessment of uninfected and infected A. anophagefferens helped link ecological relevance to physiological changes. While increases in cell size did not affect sinking velocity, viral infection increased vertical transport and suggests an increased rate of export from the water column. Notably, this was not the result of aggregation of cells through production of any extracellular polysaccharide complexes according to FlowCam measurements. An interesting question that arises from the export of virally infected cells is whether the behavior is a result of viral activity inside the virocell or is instead host driven. One possibility is the increased production of high density viral proteins (Fischer et al., 2004; Liu et al., 2022) increases density within the virocell, expediting sinking. Yet there was no significant increase in sinking velocity during later stages of infection (when virus proteins are more abundant within the cell) relative to the early (2h) stage. A contrasting hypothesis is that infected A. anophagefferens cells are exported from the water column through metabolic shifts following infection. This would create a separation between uninfected cells and new viruses released into the water column (an innate defense



A simplified p53/cell cycle checkpoint pathway based on differential transcription of *A. anophagefferens* genes during viral infection. Genes present in the *A. anophagefferens* genome are indicated in boxes with solid outlines. Other genes not known to be encoded by *A. anophagefferens* or downstream effects of a certain pathway are in boxes with dashed outlines. Upregulation in samples is indicated by red boxes and downregulation is indicated by blue boxes, with the three boxes above each respective gene corresponding to their expression versus control samples during the late day, early night, and late night. Promotion of a gene/pathway is indicated by an arrow while inhibition is indicated by blunt arrows. Pathway is based on KEGG pathways map04110 and map04115.

against community infection). Moreover, given the reduced efficiency of AaV infection on *A. anophagefferens* in the dark (Gann et al., 2020a), the expediated sinking could foster an opportunity for survival against infection, giving cellular mechanisms a chance to purge the virus or enter a cyst-like state and prevent viral

propagation (Ma et al., 2020). It is yet unclear if entering this resting stage has such an effect or if the lytic cycle continues once the cell is metabolically active again. This manifestation of the "virus shuttle" (Sullivan et al., 2017) provides a selective mechanism for reinforcement at evolutionary scales. Likewise, *A. anophagefferens*'

predilection for growth at low light may be an evolutionary adaptation to growth in the presence of viral particles (MacIntyre et al., 2004). Thus, export of virocells into the microphytobenthos may bolster a bloom in the pelagic zone where upwelling is low and residence time is high (MacIntyre et al., 2004).

Considerations for environmental sampling and diel cycles

This study illustrates the importance of sampling phototrophs throughout the solar day. Clear physiological and transcriptional differences were evident among A. anophagefferens cells depending on light history. Moreover viral transcripts in field samples have been tied to different stages of the diel cycle, with reads decreasing 10-fold between day samples and night samples on a viral species, but not genus level (Martinez-Hernandez et al., 2020) - to this end perhaps our observations should not be surprising. Yet this becomes an important caveat in the analysis of environmental-omics. Over 1,800 genes in uninfected cells were differentially expressed between at least two sampling points, corresponding to ~11% of all predicted genes in A. anophagefferens (Gann et al., 2022). Such heterogeneity in transcript abundance among control samples is compelling and indicates that cells in non-synchronous infections transcriptionally and metabolically distinct at different times of day. Yet some of the signal is also due to virus-shaped metabolism: if light shapes responses in the field as it has in our lab study, it means that when a significant portion of the population is infected (e.g., up to 37.5%, Gastrich et al., 2004) that large degrees of variability in the data could simply be the infected vs non-infected state.

Conclusion

We have demonstrated the effects of the diel cycle on growth and division of the pelagophyte A. anophagefferens and that infection by a "giant virus," Kratosvirus quantuckense strain AaV, inhibits the diel cycling of cell size and cell division. Our findings demonstrate an important linkage between cellular energetics and physiology and that this process is interrupted by viral takeover. These findings also illustrate the importance of light in the infection cycle of viruses of phototrophic hosts. When considering the activity of marine viruses, it may become important to consider sampling multiple times throughout both the day and night to achieve a higher resolution on environmental viral infection. Likewise, ignoring virocells leaves large holes in measurements of ecological physiology. Further analysis into the transcriptome of individual cells (i.e., single cell transcriptomics) in the presence and absence of infectious particles may better show the extent to which these cells vary throughout something as simple as the diel cycle. Still, our findings have revealed a continuously altering physiological profile in algae which likely extends beyond light into other environmental stimuli that should be further explored on an in situ basis.

References

Aylward, F. O., Eppley, J. M., Smith, J. M., Chavez, F. P., Scholin, C. A., and DeLong, E. F. (2015). Microbial community transcriptional networks are conserved in three domains at ocean basin scales. *Proc. Natl. Acad. Sci. USA* 112, 5443–5448. doi: 10.1073/pnas.1502883112

Data availability statement

The datasets presented in this study can be found in online repositories. The names of the repository/repositories and accession number(s) can be found in the article/Supplementary material.

Author contributions

AT: Conceptualization, Formal analysis, Investigation, Writing – original draft, Writing – review & editing. EC: Conceptualization, Formal analysis, Investigation, Writing – original draft, Writing – review & editing. AS: Investigation, Writing – review & editing. SW: Conceptualization, Supervision, Writing – review & editing.

Funding

The author(s) declare that financial support was received for the research, authorship, and/or publication of this article. This work was supported by the Simons Foundation (735077) and funds from the National Science Foundation (IOS1922958). AS was supported by a REU Site Award (NSF 2050743).

Acknowledgments

We thank Dr. Brittany Zepernick, Dr. Naomi Gilbert, Dr. Robbie Martin, Dr. Gary LeCleir, Laura Smith, and David Niknejad for their contributions and valuable discussions.

Conflict of interest

The authors declare that the research was conducted in the absence of any commercial or financial relationships that could be construed as a potential conflict of interest.

Publisher's note

All claims expressed in this article are solely those of the authors and do not necessarily represent those of their affiliated organizations, or those of the publisher, the editors and the reviewers. Any product that may be evaluated in this article, or claim that may be made by its manufacturer, is not guaranteed or endorsed by the publisher.

Supplementary material

The Supplementary material for this article can be found online at: https://www.frontiersin.org/articles/10.3389/fmicb.2024.1426193/full#supplementary-material

Babicki, S., Arndt, D., Marcu, A., Liang, Y., Grant, J. R., Maciejewski, A., et al. (2016). Heatmapper: web-enabled heat mapping for all. *Nucleic Acids Res.* 44, W147–W153. doi: 10.1093/nar/gkw419

- Beel, B., Prager, K., Spexard, M., Sasso, S., Weiss, D., Müller, N., et al. (2012). A flavin binding cryptochrome photoreceptor responds to both blue and red light in *Chlamydomonas reinhardtii*. *Plant Cell* 24, 2992–3008. doi: 10.1105/tpc.112.098947
- Behrenfeld, M. J., Prasil, O., Babin, M., and Bruyant, F. (2004). In search of a physiological basis for covariations in light-limited and light-saturated photosynthesis. *J. Phycol.* 40, 4–25. doi: 10.1046/j.1529-8817.2004.03083.x
- Beketova, E., Owens, J. L., Asberry, A. M., and Hu, C. D. (2022). PRMT5: a putative oncogene and therapeutic target in prostate cancer. *Cancer Gene Ther.* 29, 264–276. doi: 10.1038/s41417-021-00327-3
- Bienfang, P. K. (1981). SETCOL—A technologically simple and reliable method for measuring phytoplankton sinking rates. *Can. J. Fish. Aquat. Sci.* 38, 1289–1294. doi: 10.1139/f81-173
- Breker, M., Lieberman, K., and Cross, F. R. (2018). Comprehensive discovery of cell-cycle-essential pathways in *Chlamydomonas reinhardtii*. *Plant Cell* 30, 1178–1198. doi: 10.1105/tpc.18.00071
- Bricelj, V. M., and Lonsdale, D. J. (1997). *Aureococcus anophagefferens*: causes and ecological consequences of brown tides in U.S. mid-Atlantic coastal waters. *Limnol. Oceanogr.* 42, 1023–1038. doi: 10.4319/lo.1997.42.5_part_2.1023
- Brussaard, C. P. D., Kempers, R. S., Kop, A. J., Riegman, R., and Heldal, M. (1996). Virus like particles in a summer bloom of *Emiliania huxleyi* in the North Sea. *Aquat. Microb. Ecol.* 10, 105–113. doi: 10.3354/ame010105
- Brussaard, C. P. D., Kuipers, B., and Veldhuis, M. J. W. (2005). A mesocosm study of *Phaeocystis globosa* population dynamics. *Harmful Algae* 4, 859–874. doi: 10.1016/j. hal.2004.12.015
- Chase, E. E., Truchon, A. R., Coy, S. R., and Wilhelm, S. W. (2023). Aureococcus anophagefferens Virus (AaV)/*Kratosvirus quantuckense* viral particle count by SYBR Green staining and flow cytometry (CytoFLEX S Flow Cytometer Beckman Coulter). protocols.io.https://dx.doi.org/10.17504/protocols.io.dm6gpj331gzp/v2.
- Chase, E. E., Truchon, A. R., and Wilhelm, S. W. (2022). *Aureococcus anophagefferens* population count, and relative size (Violet SSC) by flow cytometry (CytoFLEX S Flow Cytometer Beckman Coulter). protocols.io https://dx.doi.org/10.17504/protocols.io.q26g7yby9gwz/v1.
- Chen, L., Bellone, R. R., Wang, Y., Singer-Berk, M., Sugasawa, K., Ford, J. M., et al. (2021). A novel DDB2 mutation causes defective recognition of UV-induced DNA damages and prevalent equine squamous cell carcinoma. *DNA Repair* 97:103022. doi: 10.1016/j.dnarep.2020.103022
- Chen, S., Lees-Miller, J. P., He, Y., and Lees-Miller, S. P. (2021). Structural insights into the role of DNA-PK as a master regulator in NHEJ. *Genome Instab. Dis.* 2, 195–210. doi: 10.1007/s42764-021-00047-w
- Chioccioli, M., Hankamer, B., and Ross, I. L. (2014). Flow cytometry pulse width data enables rapid and sensitive estimation of biomass dry weight in the microalgae *Chlamydomonas reinhardtii* and *Chlorella vulgaris*. *PLoS One* 9:e97269. doi: 10.1371/journal.pone.0097269
- Clarke, K. R. A. (2015). PRIMER v7: User Manual/Tutorial. Plymouth: PRIMER-E.
- Coesel, S., Mangogna, M., Ishikawa, T., Heijde, M., Rogato, A., Finazzi, G., et al. (2009). Diatom PtCPF1 is a new cryptochrome/photolyase family member with DNA repair and transcription regulation activity. *EMBO Rep.* 10, 655–661. doi: 10.1038/embor.2009.59
- Connell, C. M., Shibata, A., Tookman, L. A., Archibald, K. M., Flak, M. B., Pirlo, K. J., et al. (2011). Genomic DNA damage and ATR-Chk1 signaling determine oncolytic adenoviral efficacy in human ovarian cancer cells. *J. Clin. Invest.* 121, 1283–1297. doi: 10.1172/jci43976
- Coy, S. R., and Wilhelm, S. W. (2020). Concentrating viruses by tangential flow filtration. protocols.io https://dx.doi.org/10.17504/protocols.io.bbagiibw.
- Derelle, E., Yau, S., Moreau, H., and Grimsley, N. H. (2018). Prasinovirus attack of *Ostreococcus* is furtive by day but savage by night. *J. Virol.* 92:703. doi: 10.1128/JVI.01703-17
- Détain, A., Redecker, D., Leborgne-Castel, N., and Ochatt, S. (2021). Structural conservation of WEE1 and its role in cell cycle regulation in plants. $Sci.\ Rep.\ 11:23862.$ doi: 10.1038/s41598-021-03268-x
- Doty, M. S. (1959). Phytoplankton photosynthetic periodicity as a function of latitude. J. Marine Biol. Assoc. India 1, 66-68.
- Emmett, S. R., Dove, B., Mahoney, L., Wurm, T., and Hiscox, J. A. (2005). The cell cycle and virus infection. *Methods Mol. Biol.* 296, 197–218. doi: 10.1385/1-59259-857-9:197
- Fischer, H., Polikarpov, I., and Craievich, A. F. (2004). Average protein density is a molecular-weight-dependent function. *Protein Sci.* 13, 2825–2828. doi: 10.1110/ps.04688204
- Flemington, E. K. (2001). Herpesvirus lytic replication and the cell cycle: arresting new developments. J. Virol. 75, 4475–4481. doi: 10.1128/jvi.75.10.4475-4481.2001
- Frew, I. J., Dickins, R. A., Cuddihy, A. R., Del Rosario, M., Reinhard, C., O'Connell, M. J., et al. (2002). Normal p53 function in primary cells deficient for *Siah* genes. *Mol. Cell. Biol.* 22, 8155–8164. doi: 10.1128/mcb.22.23.8155-8164.2002
- Gann, E. R. (2016). ASP $_{12}$ A recipe for culturing Aureococcus anophagefferens. protocols.io https://dx.doi.org/10.17504/protocols.io.f3ybqpw.

- Gann, E. R., Gainer, P. J., Reynolds, T. B., and Wilhelm, S. W. (2020a). Influence of light on the infection of *Aureococcus anophagefferens* CCMP 1984 by a "giant virus". *PLoS One* 15:e0226758. doi: 10.1371/journal.pone.0226758
- Gann, E. R., Hughes, B. J., Reynolds, T. B., and Wilhelm, S. W. (2020b). Internal nitrogen pools shape the infection of *Aureococcus anophagefferens* CCMP 1984 by a giant virus. *Front. Microbiol.* 11:492. doi: 10.3389/fmicb.2020.00492
- Gann, E. R., Truchon, A. R., Papoulis, S. E., Dyhrman, S. T., Gobler, C. J., and Wilhelm, S. W. (2022). *Aureococcus anophagefferens* (*Pelagophyceae*) genomes improve evaluation of nutrient acquisition strategies involved in brown tide dynamics. *J. Phycol.* 58, 146–160. doi: 10.1111/jpy.13221
- Gastrich, M. D., Leigh-Bell, J. A., Gobler, C. J., Roger Anderson, O., Wilhelm, S. W., and Bryan, M. (2004). Viruses as potential regulators of regional brown tide blooms caused by the alga *Aureococcus anophagefferens*. *Estuaries* 27, 112–119. doi: 10.1007/BF02803565
- Gobler, C. J., Anderson, O. R., Gastrich, M. D., and Wilhelm, S. W. (2007). Ecological aspects of viral infection and lysis in the harmful brown tide alga *Aureococcus anophagefferens*. *Aquat. Microb. Ecol.* 47, 25–36. doi: 10.3354/ame047025
- Gobler, C. J., Lonsdale, D. J., and Boyer, G. L. (2005). A review of the causes, effects, and potential management of harmful brown tide blooms caused by *Aureococcus anophagefferens* (Hargraves et Sieburth). *Estuaries* 28, 726–749. doi: 10.1007/BF02732911
- Goto, K., and Johnson, C. H. (1995). Is the cell division cycle gated by a circadian clock? The case of *Chlamydomonas reinhardtii*. *J. Cell Biol.* 129, 1061–1069. doi: 10.1083/jcb.129.4.1061
- Groussman, R. D., Coesel, S. N., Durham, B. P., and Armbrust, E. V. (2021). Dielregulated transcriptional cascades of microbial eukaryotes in the North Pacific Subtropical Gyre. *Front. Microbiol.* 12:682651. doi: 10.3389/fmicb.2021.682651
- Gupta, S. K., Gandham, R. K., Sahoo, A. P., and Tiwari, A. K. (2015). Viral genes as oncolytic agents for cancer therapy. *Cell. Mol. Life Sci.* 72, 1073–1094. doi: 10.1007/s00018-014-1782-1
- Harding, L. W., Meeson, B. W., Prézelin, B. B., and Sweeney, B. M. (1981). Diel periodicity of photosynthesis in marine phytoplankton. *Mar. Biol.* 61, 95–105. doi: 10.1007/BF00386649
- Hastings, J. W., Astrachan, L., and Sweeney, B. M. (1961). A persistent daily rhythm in photosynthesis. *J. Gen. Physiol.* 45, 69–76. doi: 10.1085/jgp.45.1.69
- Heijde, M., Zabulon, G., Corellou, F., Ishikawa, T., Brazard, J., Usman, A., et al. (2010). Characterization of two members of the cryptochrome/photolyase family from *Ostreococcus tauri* provides insights into the origin and evolution of cryptochromes. *Plant Cell Environ.* 33, 1614–1626. doi: 10.1111/j.1365-3040.2010.02168.x
- Henderikx Freitas, F., Dugenne, M., Ribalet, F., Hynes, A., Barone, B., Karl, D. M., et al. (2020). Diel variability of bulk optical properties associated with the growth and division of small phytoplankton in the North Pacific Subtropical Gyre. *Appl. Opt.* 59, 6702–6716. doi: 10.1364/AO.394123
- Hirano, T. (2012). Condensins: universal organizers of chromosomes with diverse functions. Genes Dev. 26, 1659–1678. doi: 10.1101/gad.194746.112
- Hlavová, M., Čížková, M., Vítová, M., Bišová, K., and Zachleder, V. (2011). DNA damage during G2 phase does not affect cell cycle progression of the green alga Scenedesmus quadricauda. PLoS One 6:e19626. doi: 10.1371/journal.pone.0019626
- Holmes, R. W., and Haxo, F. T. (1958). Diurnal variations in the photosynthesis of natural phytoplankton populations in artificial light. *Special Sci. Rep. Fish.* 279, 73–76.
- Hu, S. K., Connell, P. E., Mesrop, L. Y., and Caron, D. A. (2018). A hard day's night: diel shifts in microbial eukaryotic activity in the North Pacific Subtropical Gyre. *Front. Mar. Sci.* 5:351. doi: 10.3389/fmars.2018.00351
- Jacobsen, A., and Veldhuis, M. J. W. (2005). Growth characteristics of flagellated cells of *Phaeocystis pouchetii* revealed by diel changes in cellular DNA content. *Harmful Algae* 4, 811–821. doi: 10.1016/j.hal.2004.12.001
- Jacquet, S., Heldal, M., Iglesias-Rodriguez, D., Larsen, A., Wilson, W., and Bratbak, G. (2002). Flow cytometric analysis of an *Emiliana huxleyi* bloom terminated by viral infection. *Aquat. Microb. Ecol.* 27, 111–124. doi: 10.3354/ame027111
- Jia, L., Bickel, J. S., Wu, J., Morgan, M. A., Li, H., Yang, J., et al. (2011). RBX1 (RING box protein 1) E3 ubiquitin ligase is required for genomic integrity by modulating DNA replication licensing proteins. *J. Biol. Chem.* 286, 3379–3386. doi: 10.1074/jbc. M110.188425
- Latasa, M., Cabello, A. M., Morán, X. A. G., Massana, R., and Scharek, R. (2017). Distribution of phytoplankton groups within the deep chlorophyll maximum. *Limnol. Oceanogr.* 62, 665–685. doi: 10.1002/lno.10452
- Leonard, J., Sen, N., Torres, R., Sutani, T., Jarmuz, A., Shirahige, K., et al. (2015). Condensin relocalization from centromeres to chromosome arms promotes top2 recruitment during anaphase. *Cell Rep.* 13, 2336–2344. doi: 10.1016/j.celrep.2015.11.041
- Li, X., Yu, Y., Lang, F., Chen, G., Wang, E., Li, L., et al. (2021). Cohesin promotes HSV-1 lytic transcription by facilitating the binding of RNA pol II on viral genes. *Virol. J.* 18:26. doi: 10.1186/s12985-021-01495-2
- Liu, J., Jiao, N., Hong, H., Luo, T., and Cai, H. (2005). Proliferating cell nuclear antigen (PCNA) as a marker of cell proliferation in the marine dinoflagellate *Prorocentrum*

donghaiense Lu and the green alga Dunaliella salina Teodoresco. J. Appl. Phycol. 17, 323–330. doi: 10.1007/s10811-005-5943-3

Liu, X., Oh, S., and Kirschner, M. W. (2022). The uniformity and stability of cellular mass density in mammalian cell culture. *Front. Cell Dev. Biol.* 10:1017499. doi: 10.3389/fcell.2022.1017499

Love, M. I., Huber, W., and Anders, S. (2014). Moderated estimation of fold change and dispersion for RNA-seq data with DESeq2. *Genome Biol.* 15:550. doi: 10.1186/s13059-014-0550-8

Luserna, G., di Rorà, A., Cerchione, C., Martinelli, G., and Simonetti, G. (2020). A WEE1 family business: regulation of mitosis, cancer progression, and therapeutic target. *J. Hematol. Oncol.* 13:126. doi: 10.1186/s13045-020-00959-2

Ma, Z., Hu, Z., Deng, Y., Shang, L., Gobler, C. J., and Tang, Y. Z. (2020). Laboratory culture-based characterization of the resting stage cells of the brown-tide-causing pelagophyte, *Aureococcus anophagefferens. J. Marine Sci. Eng.* 8:1027. doi: 10.3390/imse8121027

MacIntyre, H. L., Lomas, M. W., Cornwell, J., Suggett, D. J., Gobler, C. J., Koch, E. W., et al. (2004). Mediation of benthic-pelagic coupling by microphytobenthos: an energy-and material-based model for initiation of blooms of *Aureococcus anophagefferens*. *Harmful Algae* 3, 403–437. doi: 10.1016/j.hal.2004.05.005

Mao, Y., Li, X., Zhang, G., Liao, Y., Qian, G., and Sun, J. (2021). Sinking rate and community structures of autumn phytoplankton responses to mesoscale physical processes in the Western South China Sea. *Front. Microbiol.* 12:777473. doi: 10.3389/fmicb.2021.777473

Martinez-Hernandez, F., Luo, E., Tominaga, K., Ogata, H., Yoshida, T., DeLong, E. F., et al. (2020). Diel cycling of the cosmopolitan abundant Pelagibacter virus 37-F6: one of the most abundant viruses on earth. *Environ. Microbiol. Rep.* 12, 214–219. doi: 10.1111/1758-2229.12825

Matthews, D., Emmott, E., and Hiscox, J. (2011). Viruses and the nucleolus. *Nucleolus* 15, 321–345. doi: 10.1007/978-1-4614-0514-6

Mawphlang, O. I. L., and Kharshiing, E. V. (2017). Photoreceptor mediated plant growth responses: implications for photoreceptor engineering toward improved performance in crops. *Front. Plant Sci.* 8:1181. doi: 10.3389/fpls.2017.01181

Maxwell, S. D., and Mikihiko, O. (1957). Evidence for a photosynthetic daily periodicity. *Limnol. Oceanogr.* 2, 37–40. doi: 10.4319/lo.1957.2.1.0037

McVey, M. J., Spring, C. M., and Kuebler, W. M. (2018). Improved resolution in extracellular vesicle populations using 405 instead of 488 nm side scatter. *J. Extracell Vesic.* 7:1454776. doi: 10.1080/20013078.2018.1454776

Mendenhall, M. D., and Hodge, A. E. (1998). Regulation of Cdc28 cyclin-dependent protein kinase activity during the cell cycle of the yeast *Saccharomyces cerevisiae*. *Microbiol. Mol. Biol. Rev.* 62, 1191–1243. doi: 10.1128/mmbr.62.4.1191-1243.1998

Mendoza, M., Mandani, G., and Momand, J. (2014). The MDM2 gene family. *Biomol. Concepts* 5, 9–19. doi: 10.1515/bmc-2013-0027

Moldovan, G.-L., Pfander, B., and Jentsch, S. (2007). PCNA, the maestro of the replication fork. Cell 129, 665–679. doi: 10.1016/j.cell.2007.05.003

Moniruzzaman, M., Gann, E. R., and Wilhelm, S. W. (2018). Infection by a giant virus (AaV) induces widespread physiological reprogramming in *Aureococcus anophagefferens* CCMP1984- a harmful bloom algae. *Front. Microbiol.* 9:752. doi: 10.3389/fmicb.2018.00752

Moulager, M., Monnier, A., Jesson, B. L., Bouvet, R. G., Mosser, J., Schwartz, C., et al. (2007). Light-dependent regulation of cell division in *Ostreococcus*: evidence for a major transcriptional input. *Plant Physiol.* 144, 1360–1369. doi: 10.1104/pp.107.096149

Muratore, D., Boysen, A. K., Harke, M. J., Becker, K. W., Casey, J. R., Coesel, S. N., et al. (2022). Complex marine microbial communities partition metabolism of scarce resources over the diel cycle. *Nat. Ecol. Evol.* 6, 218–229. doi: 10.1038/s41559-021-01606-w

Naghavi, M. H., and Walsh, D. (2017). Microtubule regulation and function during virus infection. *J. Virol.* 91:538. doi: 10.1128/jvi.00538-17

Nedelcu, A. M. (2006). Evidence for p53-like-mediated stress responses in green algae. FEBS Lett. 580, 3013–3017. doi: 10.1016/j.febslet.2006.04.044

Needham, D. M., Yoshizawa, S., Hosaka, T., Poirier, C., Choi, C. J., Hehenberger, E., et al. (2019). A distinct lineage of giant viruses brings a rhodopsin photosystem to unicellular marine predators. *Proc. Natl. Acad. Sci.* 116, 20574–20583. doi: 10.1073/pnas.1907517116

Nelson, D. M., and Brand, L. E. (1979). Cell division periodicity in 13 species of marine phytoplankton on a light: dark cycle. *J. Phycol.* 15, 67–75. doi: 10.1111/j.1529-8817.1979.tb02964.x

Ottesen, E. A., Young, C. R., Gifford, S. M., Eppley, J. M., Marin, R., Schuster, S. C., et al. (2014). Multispecies diel transcriptional oscillations in open ocean heterotrophic bacterial assemblages. *Science* 345, 207–212. doi: 10.1126/science.1252476

Pecani, K., Lieberman, K., Tajima-Shirasaki, N., Onishi, M., and Cross, F. R. (2022). Control of division in *Chlamydomonas* by cyclin B/CDKB1 and the anaphase-promoting complex. *PLoS Genet*. 18:e1009997. doi: 10.1371/journal.pgen.1009997

Perrin, L., Probert, I., Langer, G., and Aloisi, G. (2016). Growth of the coccolithophore *Emiliania huxleyi* in light-and nutrient-limited batch reactors: relevance for the BIOSOPE deep ecological niche of coccolithophores. *Biogeosciences* 13, 5983–6001. doi: 10.5194/bg-13-5983-2016

Peters, J. M., Tedeschi, A., and Schmitz, J. (2008). The cohesin complex and its roles in chromosome biology. *Genes Dev.* 22, 3089–3114. doi: 10.1101/gad.1724308

Petersen, J., Rredhi, A., Szyttenholm, J., Oldemeyer, S., Kottke, T., and Mittag, M. (2021). The world of algae reveals a broad variety of cryptochrome properties and functions. *Front. Plant Sci.* 12:766509. doi: 10.3389/fpls.2021.766509

Poretsky, R. S., Hewson, I., Sun, S., Allen, A. E., Zehr, J. P., and Moran, M. A. (2009). Comparative day/night metatranscriptomic analysis of microbial communities in the North Pacific Subtropical Gyre. *Environ. Microbiol.* 11, 1358–1375. doi: 10.1111/j.1462-2920.2008.01863.x

 Prezelin, B. B. (1992). Diel periodicity in phytoplankton productivity. $\it Hydrobiologia 238, 1–35.$ doi: 10.1007/BF00048771

Probyn, T. A., Bernard, S., Pitcher, G. C., and Pienaar, R. N. (2010). Ecophysiological studies on *Aureococcus anophagefferens* blooms in Saldanha Bay, South Africa. *Harmful Algae* 9, 123–133. doi: 10.1016/j.hal.2009.08.008

Rowe, J. M., Dunlap, J. R., Gobler, C. J., Anderson, O. R., Gastrich, M. D., and Wilhelm, S. W. (2008). Isolation of a non-phage-like lytic virus infecting *Aureococcus anophagefferens*. *J. Phycol.* 44, 71–76. doi: 10.1111/j.1529-8817.2007.00453.x

Sanchez-Pulido, L., and Ponting, C. P. (2011). Cdc45: the missing RecJ ortholog in eukaryotes? *Bioinformatics* 27, 1885–1888. doi: 10.1093/bioinformatics/btr332

Shimada, B. M. (1958). Diurnal fluctuation in photosynthetic rate and chlorophyll "a" content of phytoplankton from eastern Pacific waters. *Limnol. Oceanogr.* 3, 336–339. doi: 10.4319/lo.1958.3.3.0336

Shirai, Y., Tomaru, Y., Takao, Y., Suzuki, H., Nagumo, T., and Nagasaki, K. (2008). Isolation and characterization of a single-stranded RNA virus infecting the marine planktonic diatom *Chaetoceros tenuissimus* Meunier. *Appl. Environ. Microbiol.* 74, 4022–4027. doi: 10.1128/aem.00509-08

Sieburth, J. M., Johnson, P. W., and Hargraves, P. E. (1988). Ultrastructure and ecology of *Aureococcus anophagefferens* gen. *et. sp. nov.* (Chrysophyceae) - the dominant picoplankter during a bloom in Narragansett Bay, Rhode-Island, summer 1985. *J. Phycol.* 24, 416–425. doi: 10.1111/j.1529-8817.1988.tb04485.x

Skibbens, R. V. (2019). Condensins and cohesins - one of these things is not like the other! *I. Cell Sci.* 132:220491. doi: 10.1242/ics.220491

Steffen, M. M., Davis, T. W., McKay, R. M. L., Bullerjahn, G. S., Krausfeldt, L. E., Stough, J. M. A., et al. (2017). Ecophysiological examination of the Lake Erie *Microcystis* bloom in 2014: linkages between biology and the water supply shutdown of Toledo, OH. *Environ. Sci. Technol.* 51, 6745–6755. doi: 10.1021/acs.est.7b00856

Sullivan, M. B., Weitz, J. S., and Wilhelm, S. W. (2017). Viral ecology comes of age. *Environ. Microbiol. Rep.* 9, 33–35. doi: 10.1111/1758-2229.12504

Sumiya, N., Fujiwara, T., Kobayashi, Y., Misumi, O., and Miyagishima, S. Y. (2014). Development of a heat-shock inducible gene expression system in the red alga *Cyanidioschyzon merolae. PLoS One* 9:e111261. doi: 10.1371/journal.pone.0111261

Tang, K. W. (2003). Grazing and colony size development in *Phaeocystis globosa* (Prymnesiophyceae): the role of a chemical signal. *J. Plankton Res.* 25, 831–842. doi: 10.1093/plankt/25.7.831

Terhorst, A., Sandikci, A., Whittaker, C. A., Szórádi, T., Holt, L. J., Neurohr, G. E., et al. (2023). The environmental stress response regulates ribosome content in cell cycle-arrested *S. cerevisiae*. Front cell. *Dev. Biol.* 11:1118766. doi: 10.3389/fcell.2023.1118766

Truchon, A. R., Chase, E. E., Gann, E. R., Moniruzzaman, M., Creasey, B. A., Aylward, F. O., et al. (2023). *Kratosvirus quantuckense*: the history and novelty of an algal bloom disrupting virus and a model for giant virus research. *Front. Microbiol.* 14:1284617. doi: 10.3389/fmicb.2023.1284617

Vincent, F., Gralka, M., Schleyer, G., Schatz, D., Cabrera-Brufau, M., Kuhlisch, C., et al. (2023). Viral infection switches the balance between bacterial and eukaryotic recyclers of organic matter during coccolithophore blooms. *Nat. Commun.* 14:510. doi: 10.1038/s41467-023-36049-3

Vincent, F., Sheyn, U., Porat, Z., Schatz, D., and Vardi, A. (2021). Visualizing active viral infection reveals diverse cell fates in synchronized algal bloom demise. *Proc. Natl. Acad. Sci. USA* 118:e2021586118. doi: 10.1073/pnas.2021586118

Wagner, G. P., Kin, K., and Lynch, V. J. (2012). Measurement of mRNA abundance using RNA-seq data: RPKM measure is inconsistent among samples. *Theory Biosci.* 131, 281–285. doi: 10.1007/s12064-012-0162-3

Watanabe, N., Arai, H., Nishihara, Y., Taniguchi, M., Watanabe, N., Hunter, T., et al. (2004). M-phase kinases induce phospho-dependent ubiquitination of somatic Weel by SCFbeta-TrCP. *Proc. Natl. Acad. Sci. USA* 101, 4419–4424. doi: 10.1073/pnas.0307700101

Wilhelm, S. W., and Suttle, C. A. (1999). Viruses and nutrient cycles in the sea: viruses play critical roles in the structure and function of aquatic food webs. *Bioscience* 49, 781–788. doi: 10.2307/1313569

Yentsch, C. S., and Ryther, J. H. (1957). Short-term variations in phytoplankton chlorophyll and their significance. $\it Limnol.\ Oceanogr.\ 2$, 140–142. doi: 10.4319/lo.1957.2.2.0140

Yoshikawa, T., and Furuya, K. (2006). Effects of diurnal variations in phytoplankton photosynthesis obtained from natural fluorescence. *Mar. Biol.* 150, 299–311. doi: 10.1007/s00227-006-0331-3

Zhang, Q. C., Qiu, L. M., Yu, R. C., Kong, F. Z., Wang, Y. F., Yan, T., et al. (2012). Emergence of brown tides caused by *Aureococcus anophagefferens* Hargraves et Sieburth in China. *Harmful Algae* 19, 117–124. doi: 10.1016/j.hal.2012.06.007

Zhang, D., Yu, Z., Hu, S., Liu, X., Zeng, B., Gao, W., et al. (2023). Genome-wide identification of members of the Skp1 family in almond (*Prunus dulcis*), cloning and expression characterization of PsdSSK1. *Physiol. Mol. Biol. Plants* 29, 35–49. doi: 10.1007/s12298-023-01278-9

Zhao, Y., Zhao, Y., Zheng, S., Zhao, L., Zhang, W., Xiao, T., et al. (2023). Enhanced resolution of marine viruses with violet side scatter. *Cytometry A* 103, 260–268. doi: 10.1002/cyto.a.24674

Zinser, E. R., Lindell, D., Johnson, Z. I., Futschik, M. E., Steglich, C., Coleman, M. L., et al. (2009). Choreography of the transcriptome, photophysiology, and cell cycle of a minimal photoautotroph, *Prochlorococcus. PLoS One* 4:e5135. doi: 10.1371/journal.pone.0005135

Zuo, Z., Zhou, Z., Chang, Y., Liu, Y., Shen, Y., Li, Q., et al. (2024). Ribonucleotide reductase M2 (RRM2): regulation, function and targeting strategy in human cancer. *Genes Dis.* 11, 218–233. doi: 10.1016/j.gendis.2022.11.022